Electronic Supplementary Material (ESI) for Physical Chemistry Chemical Physics.

Molecular understanding of ion specificity at the peptide bond

Chuanyu Yan and Tiancheng Mu*

Department of Chemistry, Renmin University of China, Beijing 100872, P. R. China.

Correspondence should be addressed to,

E-mail: tcmu@chem.ruc.edu.cn; Fax: +86-10-62516444; Tel: +86-10-62514925

Supplementary Information

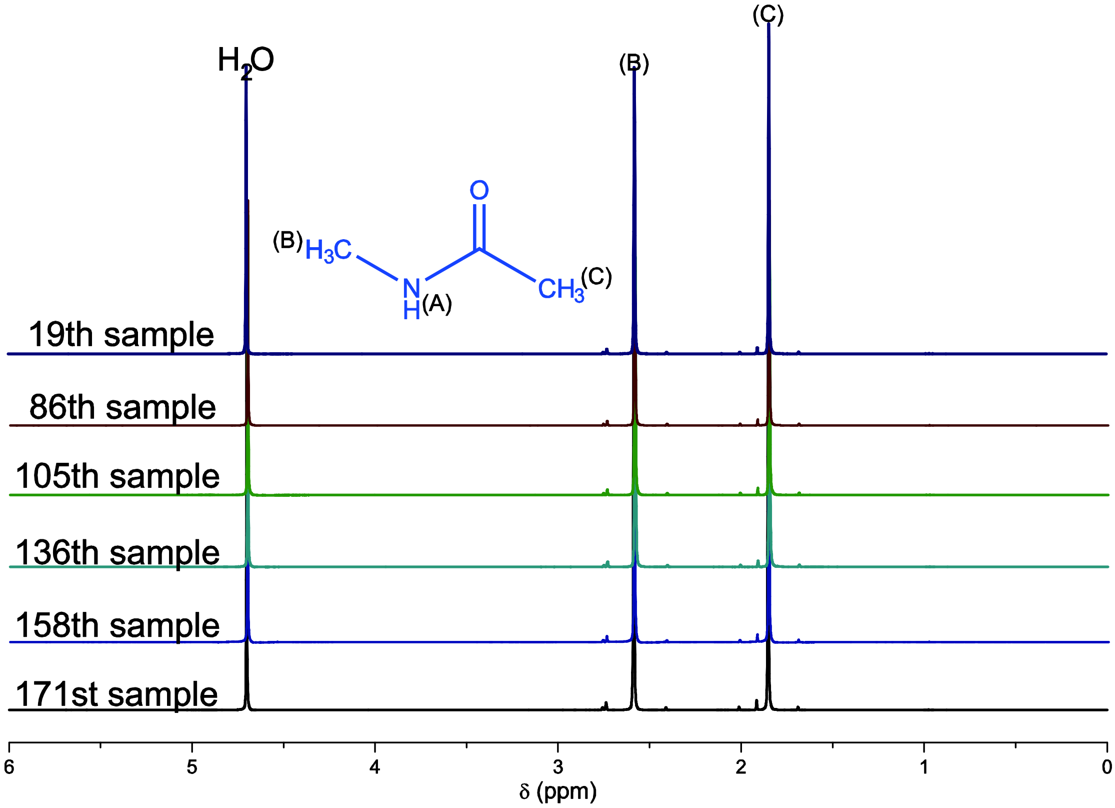

Fig. S1 ^{1}H-NMR spectra of NMA at 298.15 K. The solvent is D2O and the concentration is 0.25 M. In order to make sure that the changes in chemical shift are not affected by the instability of equipments, the ^{1}H-NMR test for bulk solutions of NMA was repeated several times among 197 NMR tests.

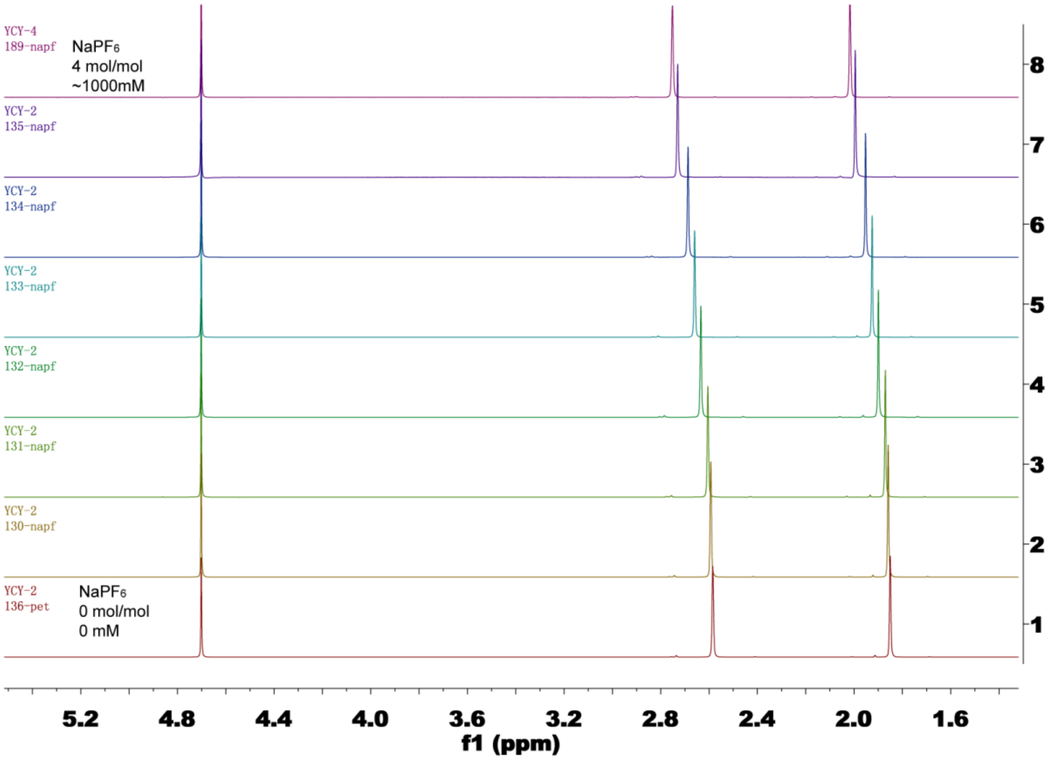

Fig. S2 Original data of $NaPF_6$ effects on NMR spectra of NMA. The concentration of NMA was constantly 0.25 M while the concentration of $NaPF_6$ in sample solutions was decreasing from upper spectra to bottom.

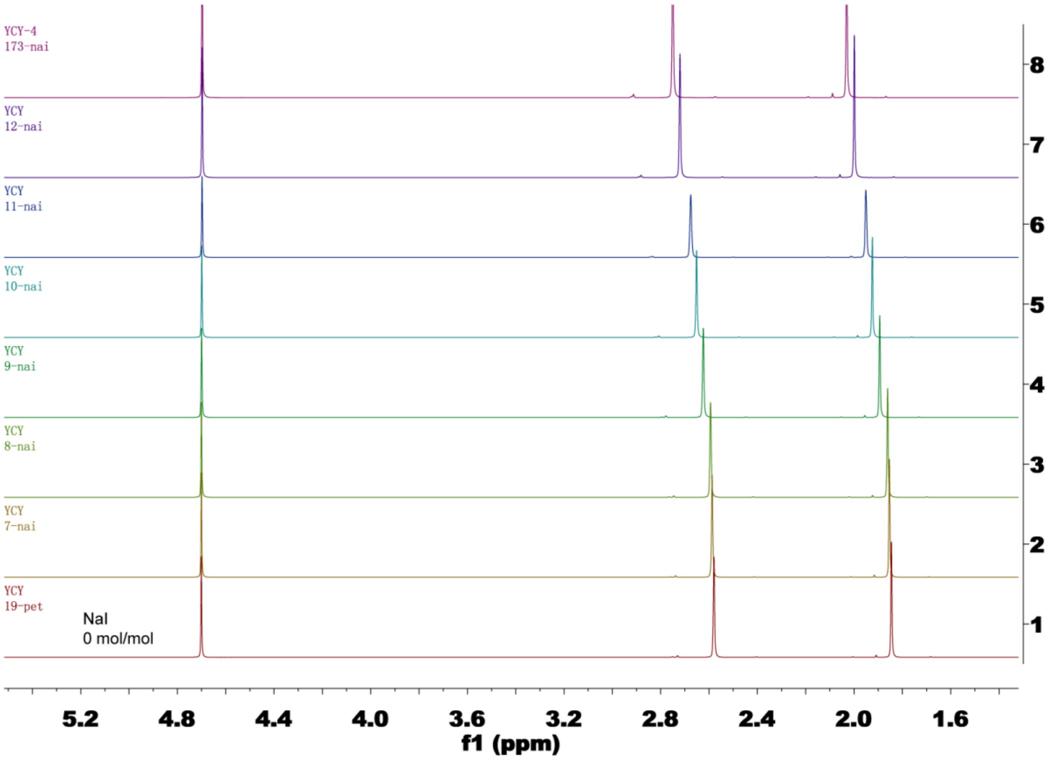

Fig. S3 Original data of NaI effects on NMR spectra of NMA. The concentration of NMA was constantly 0.25 M while the concentration of NaI in sample solutions was decreasing from upper spectra to bottom.

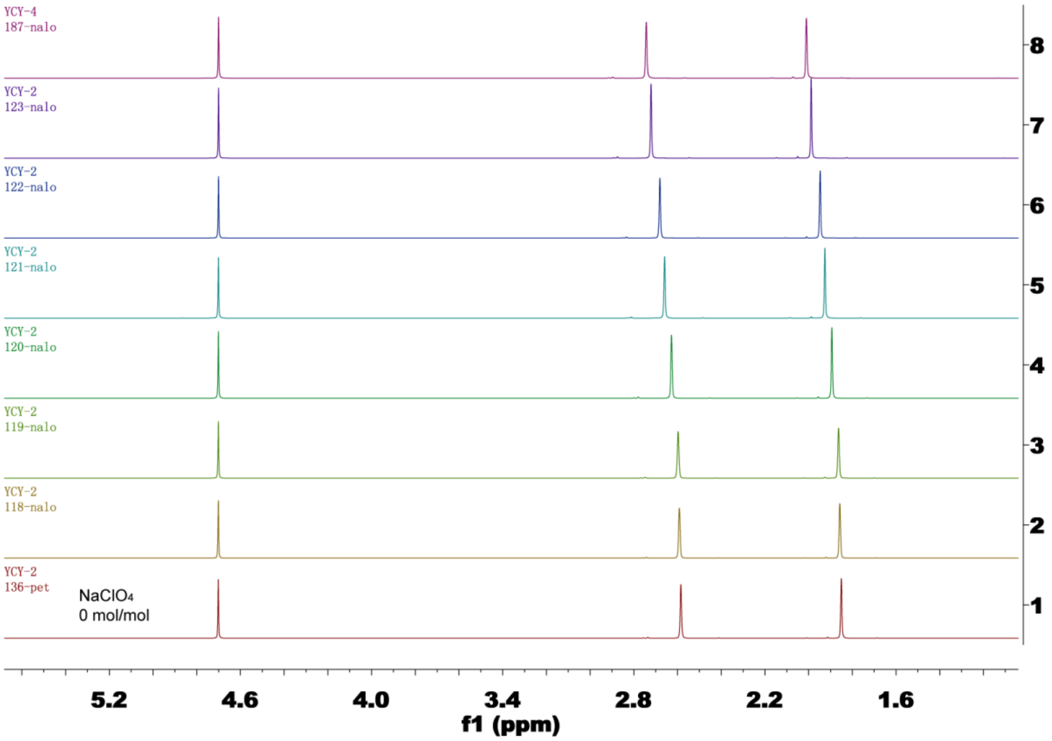

Fig. S4 Original data of $NaClO_4$ effects on NMR spectra of NMA. The concentration of NMA was constantly 0.25 M while the concentration of $NaClO_4$ in sample solutions was decreasing from upper spectra to bottom.

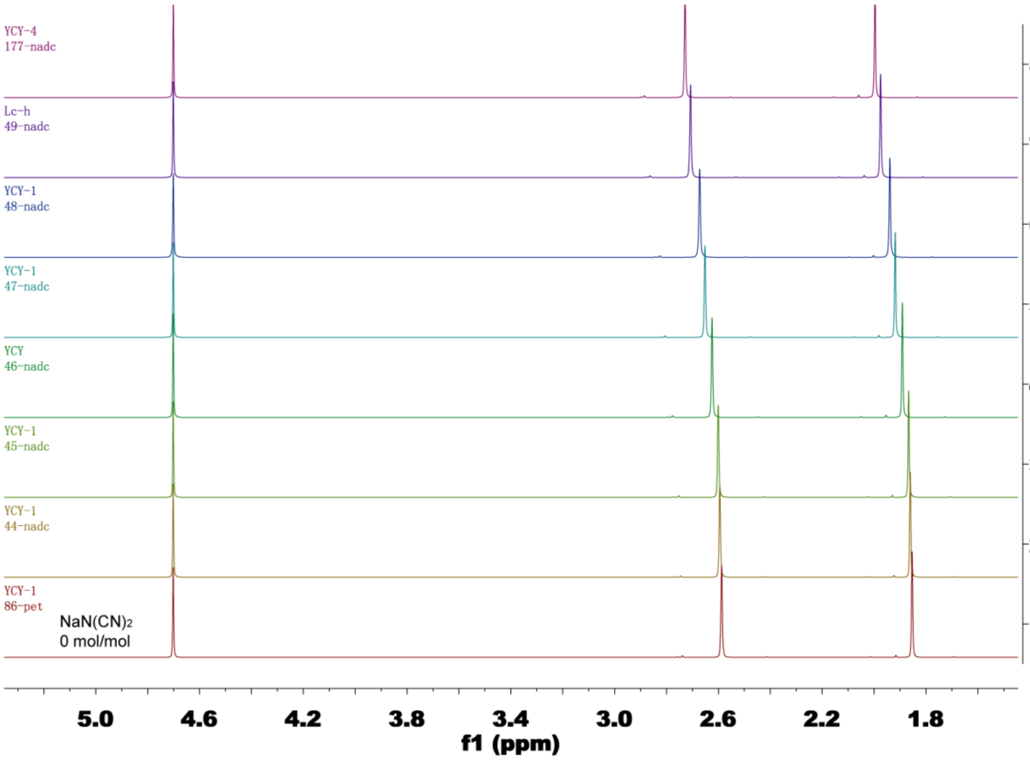

Fig. S5 Original data of $NaN(CN)_2$ effects on NMR spectra of NMA. The concentration of NMA was constantly 0.25 M while the concentration of $NaN(CN)_2$ in sample solutions was decreasing from upper spectra to bottom.

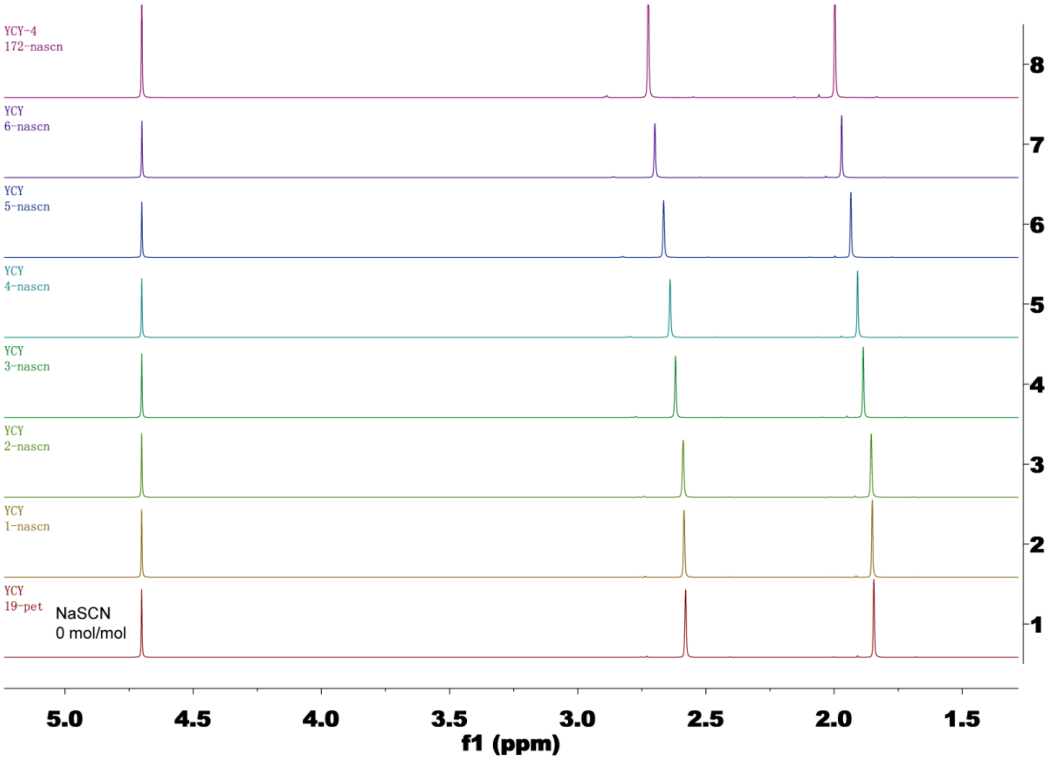

Fig. S6 Original data of NaSCN effects on NMR spectra of NMA. The concentration of NMA was constantly 0.25 M while the concentration of NaSCN in sample solutions was decreasing from upper spectra to bottom.

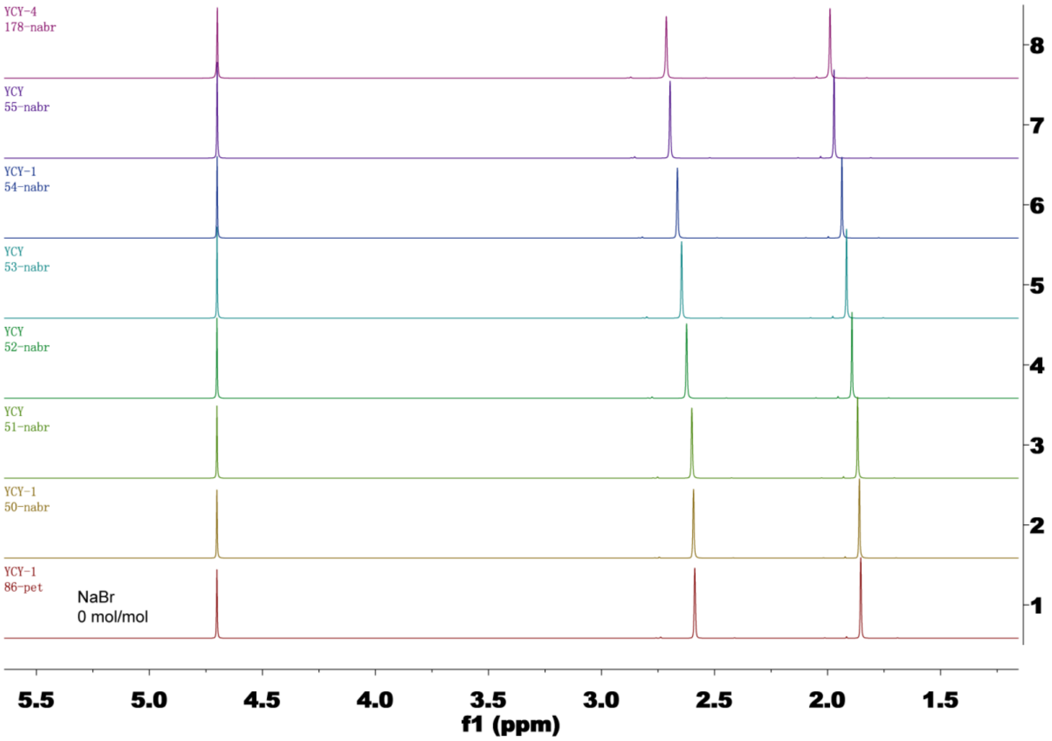

Fig. S7 Original data of NaBr effects on NMR spectra of NMA. The concentration of NMA was constantly 0.25 M while the concentration of NaBr in sample solutions was decreasing from upper spectra to bottom.

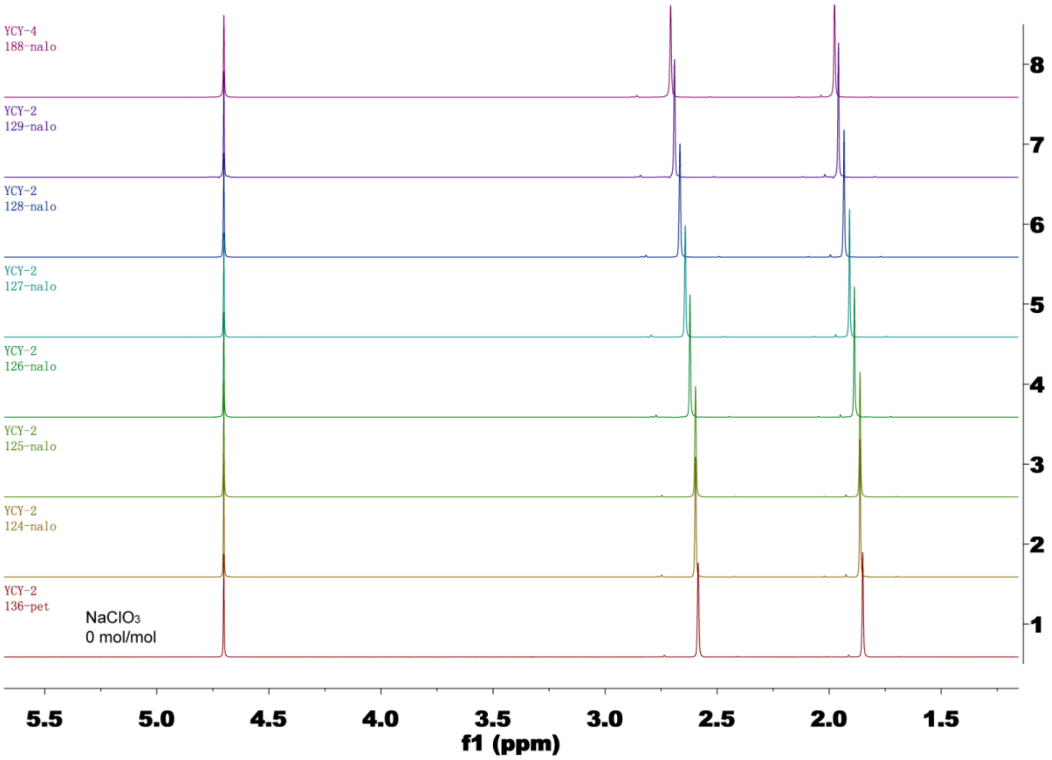

Fig. S8 Original data of $NaClO_3$ effects on NMR spectra of NMA. The concentration of NMA was constantly 0.25 M while the concentration of $NaClO_3$ in sample solutions was decreasing from upper spectra to bottom.

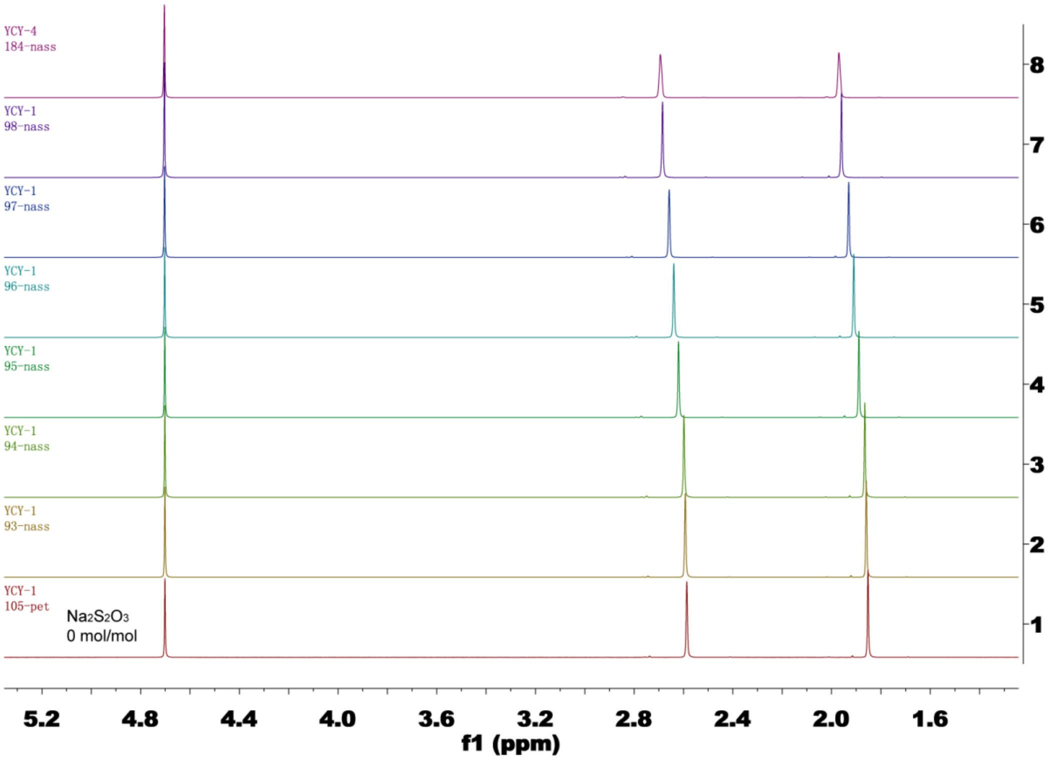

Fig. S9 Original data of $Na_2S_2O_3$ effects on NMR spectra of NMA. The concentration of NMA was constantly 0.25 M while the concentration of $NaClO_3$ in sample solutions was decreasing from upper spectra to bottom.

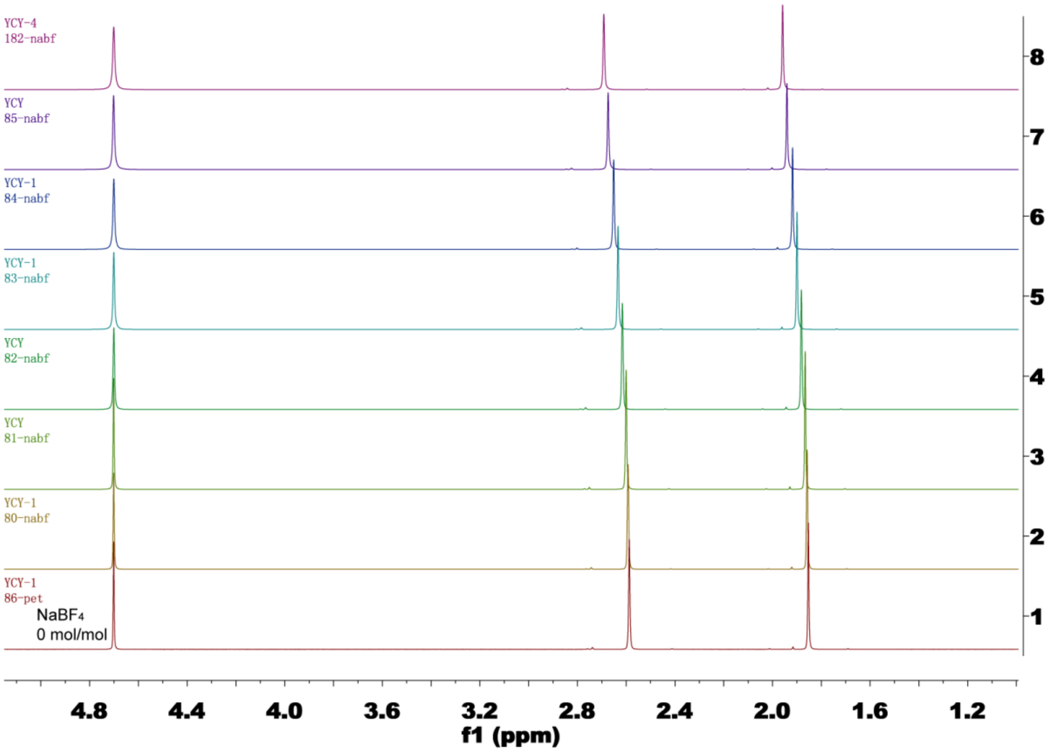

Fig. S10 Original data of $NaBF_4$ effects on NMR spectra of NMA. The concentration of NMA was constantly 0.25 M while the concentration of $NaBF_4$ in sample solutions was decreasing from upper spectra to bottom.

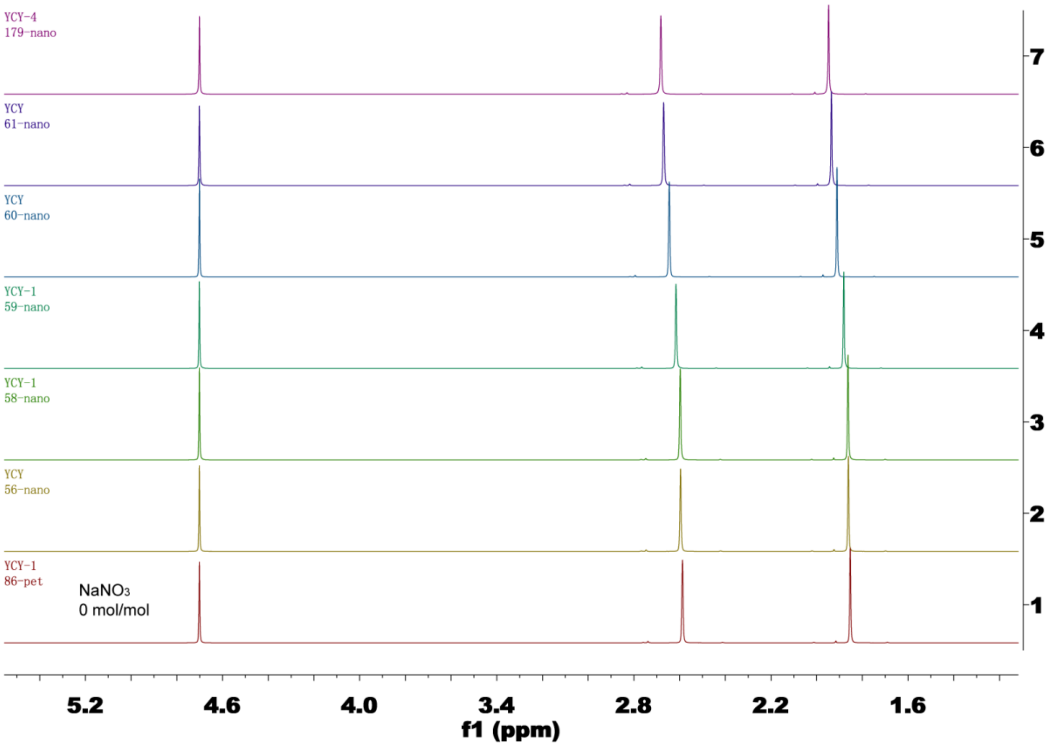

Fig. S11 Original data of $NaNO_3$ effects on NMR spectra of NMA. The concentration of NMA was constantly 0.25 M while the concentration of $NaNO_3$ in sample solutions was decreasing from upper spectra to bottom.

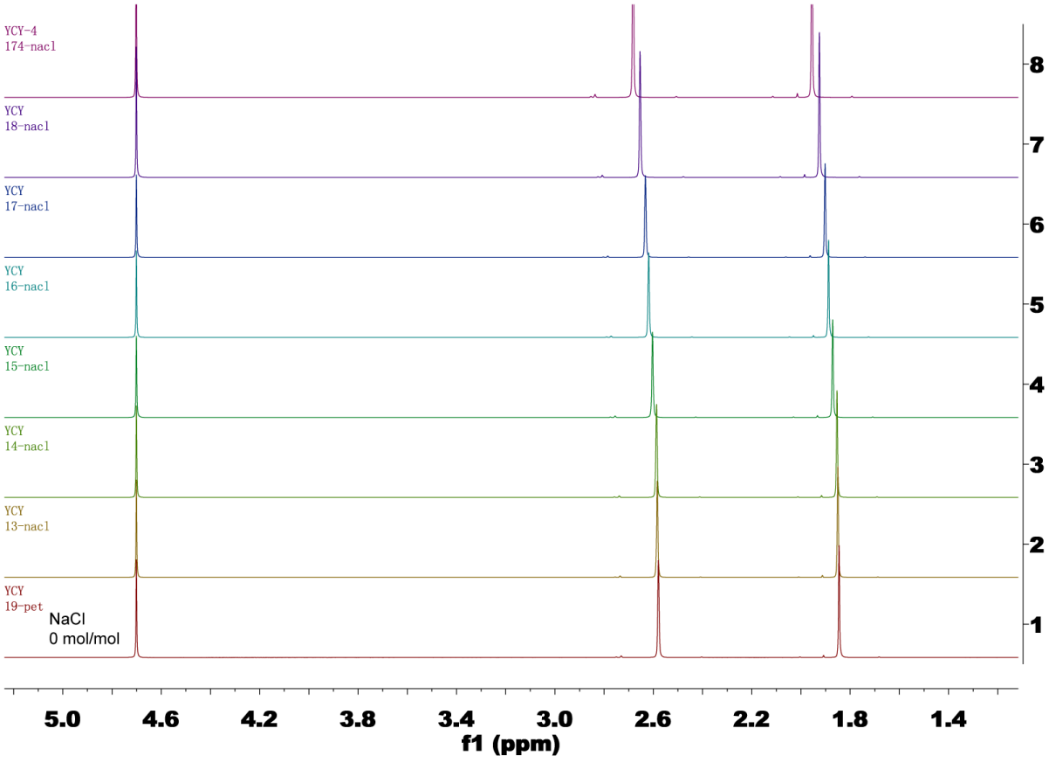

Fig. S12 Original data of NaCl effects on NMR spectra of NMA. The concentration of NMA was constantly 0.25 M while the concentration of NaCl in sample solutions was decreasing from upper spectra to bottom.

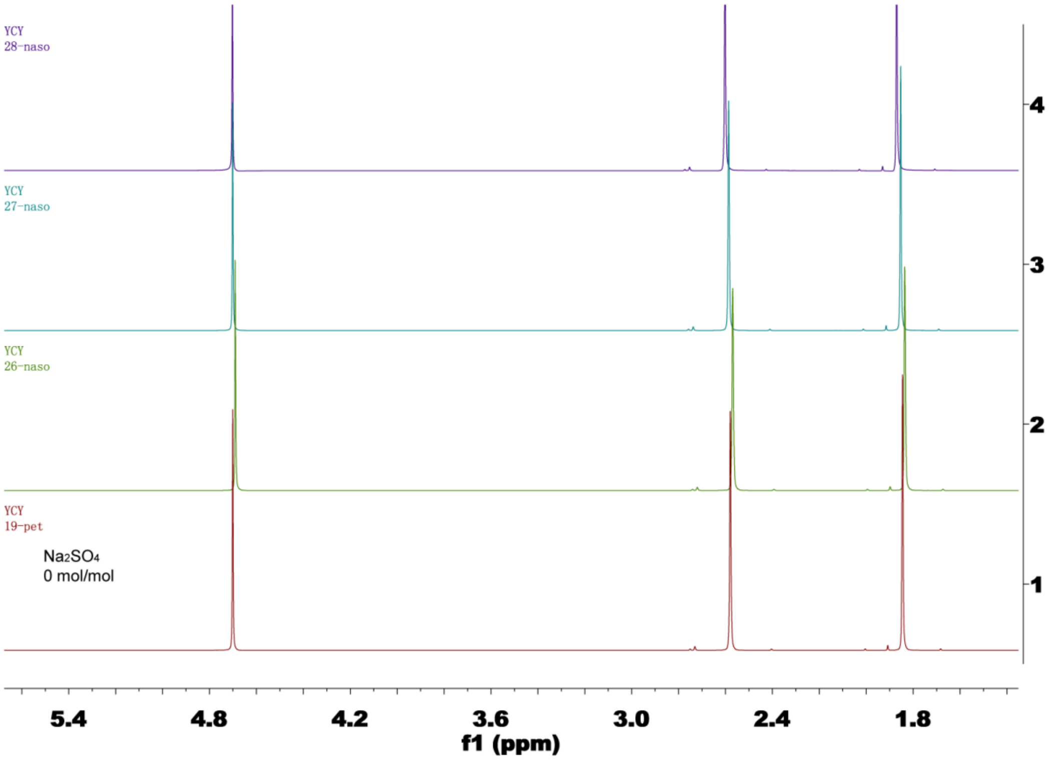

Fig. S13 Original data of Na_2SO_4 effects on NMR spectra of NMA. The concentration of NMA was constantly 0.25 M while the concentration of Na_2SO_4 in sample solutions was decreasing from upper spectra to bottom.

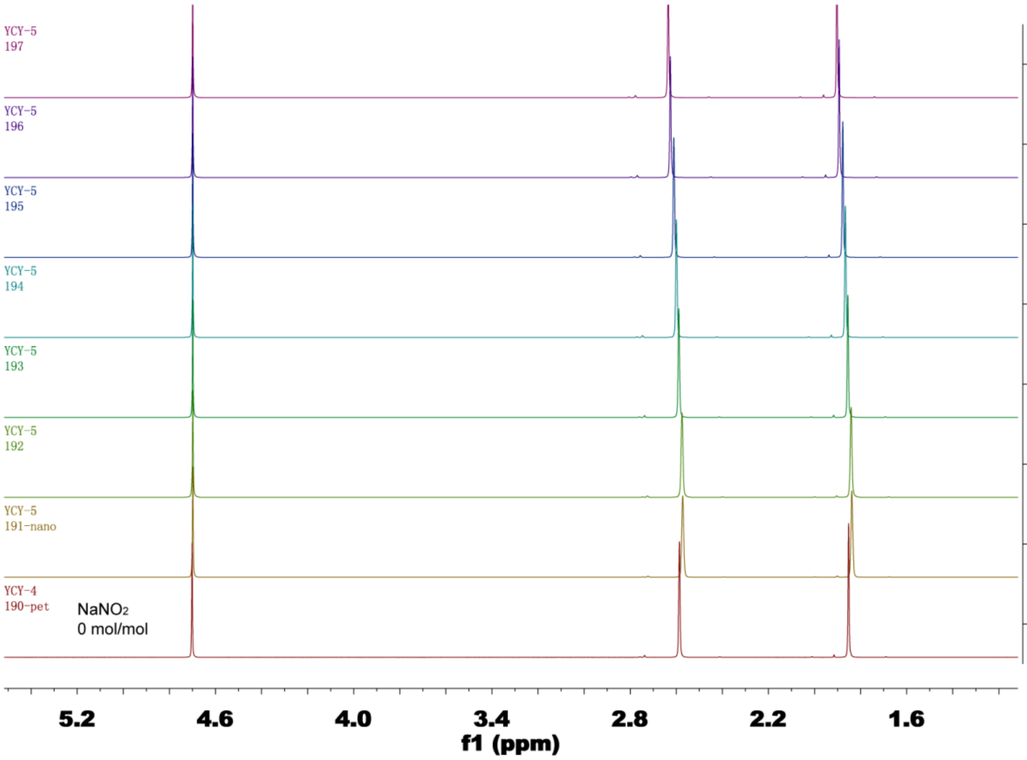

Fig. S14 Original data of $NaNO_2$ effects on NMR spectra of NMA. The concentration of NMA was constantly 0.25 M while the concentration of $NaNO_2$ in sample solutions was decreasing from upper spectra to bottom.

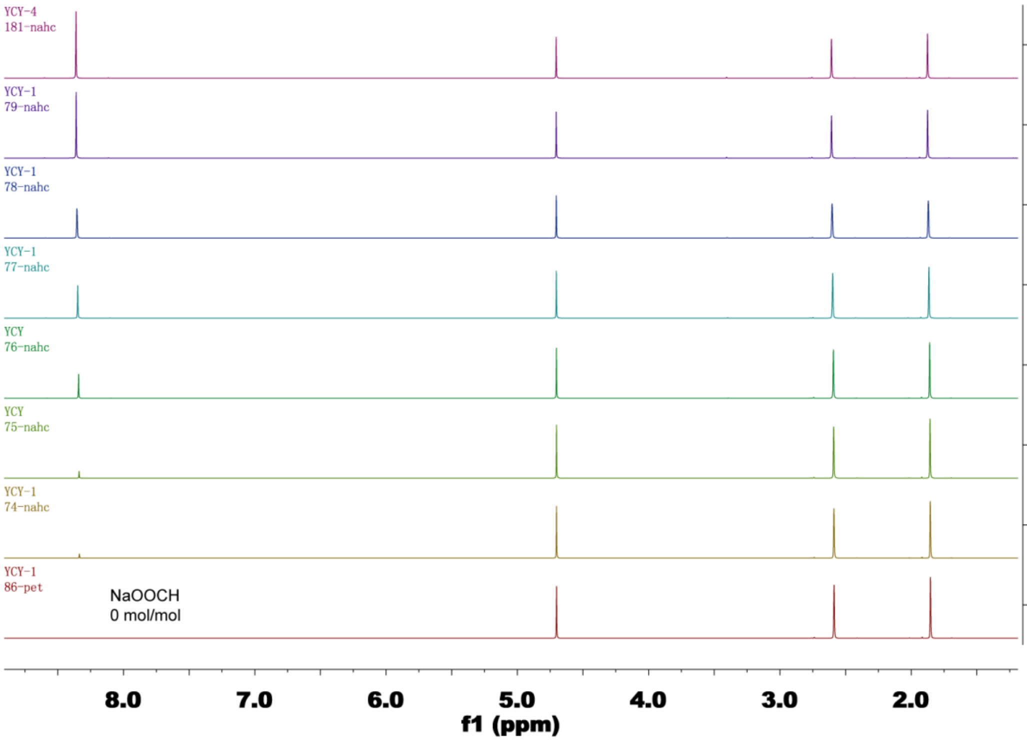

Fig. S15 Original data of NaOOCH effects on NMR spectra of NMA. The concentration of NMA was constantly 0.25 M while the concentration of NaOOCH in sample solutions was decreasing from upper spectra to bottom.

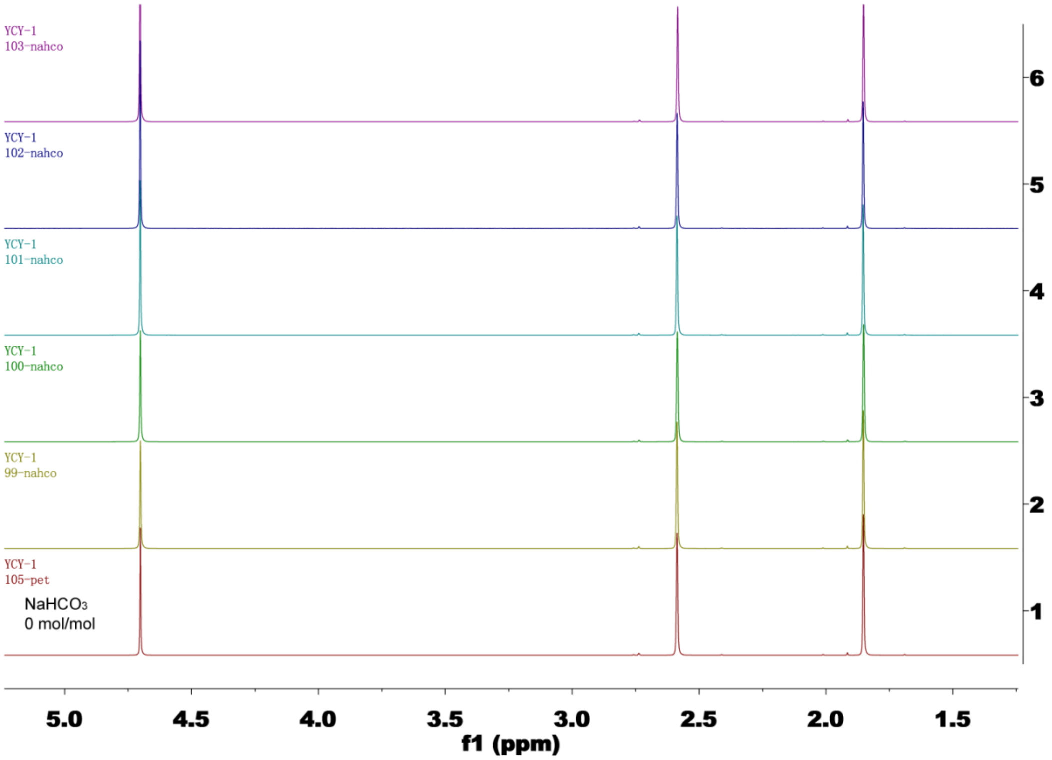

Fig. S16 Original data of $NaHCO_3$ effects on NMR spectra of NMA. The concentration of NMA was constantly 0.25 M while the concentration of $NaHCO_3$ in sample solutions was decreasing from upper spectra to bottom.

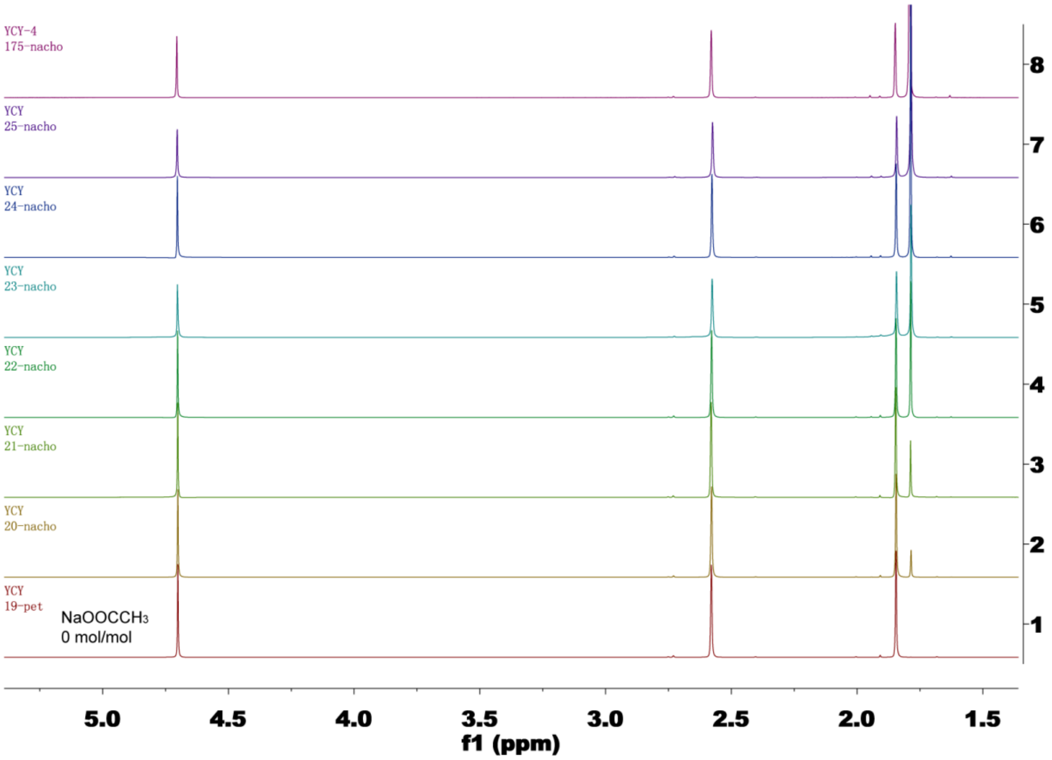

Fig. S17 Original data of $NaOOCCH_3$ effects on NMR spectra of NMA. The concentration of NMA was constantly 0.25 M while the concentration of $NaOOCCH_3$ in sample solutions was decreasing from upper spectra to bottom.

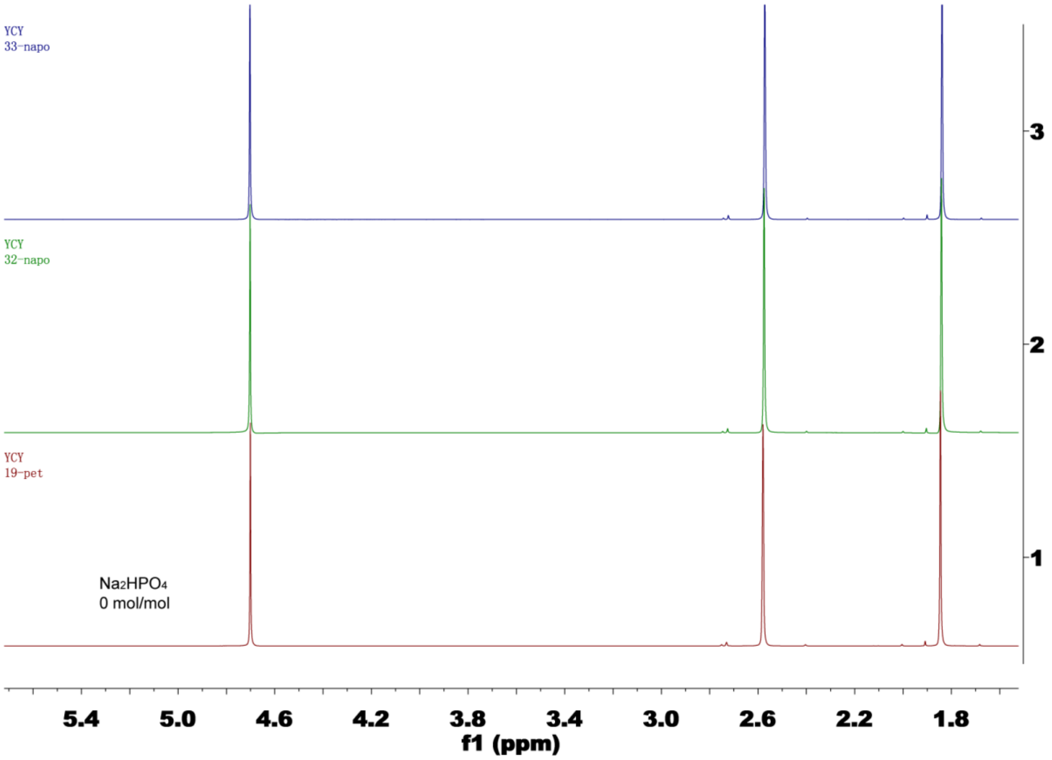

Fig. S18 Original data of Na_2HPO_4 effects on NMR spectra of NMA. The concentration of NMA was constantly 0.25 M while the concentration of Na_2HPO_4 in sample solutions was decreasing from upper spectra to bottom.

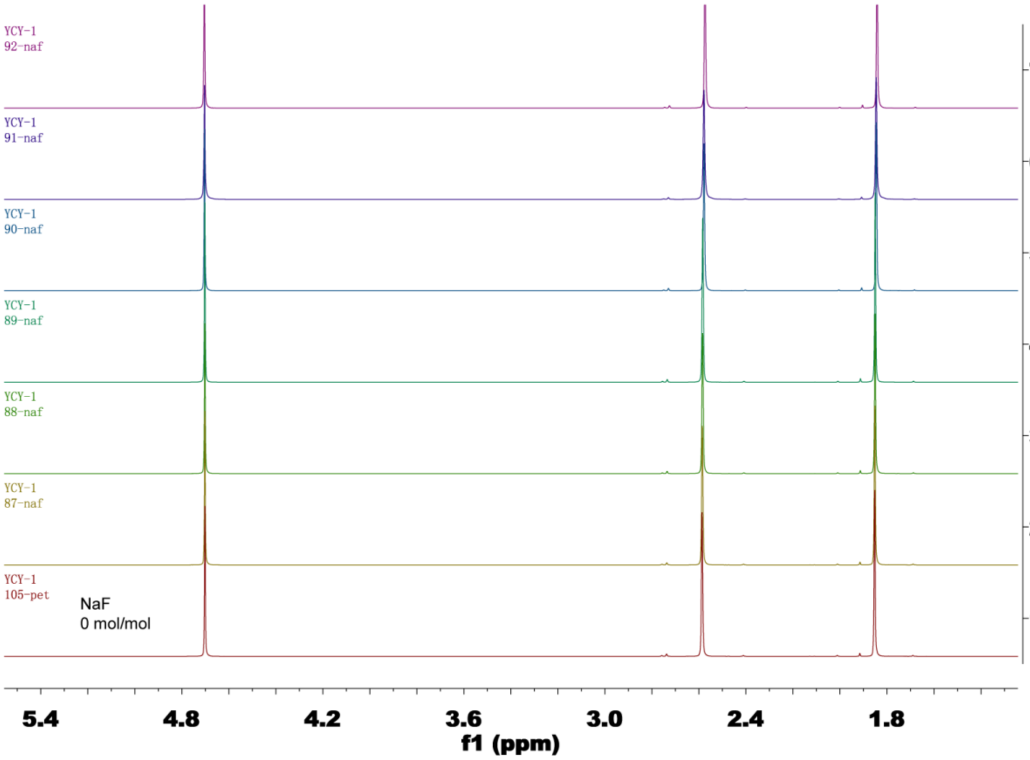

Fig. S19 Original data of NaF effects on NMR spectra of NMA. The concentration of NMA was constantly 0.25 M while the concentration of NaF in sample solutions was decreasing from upper spectra to bottom.

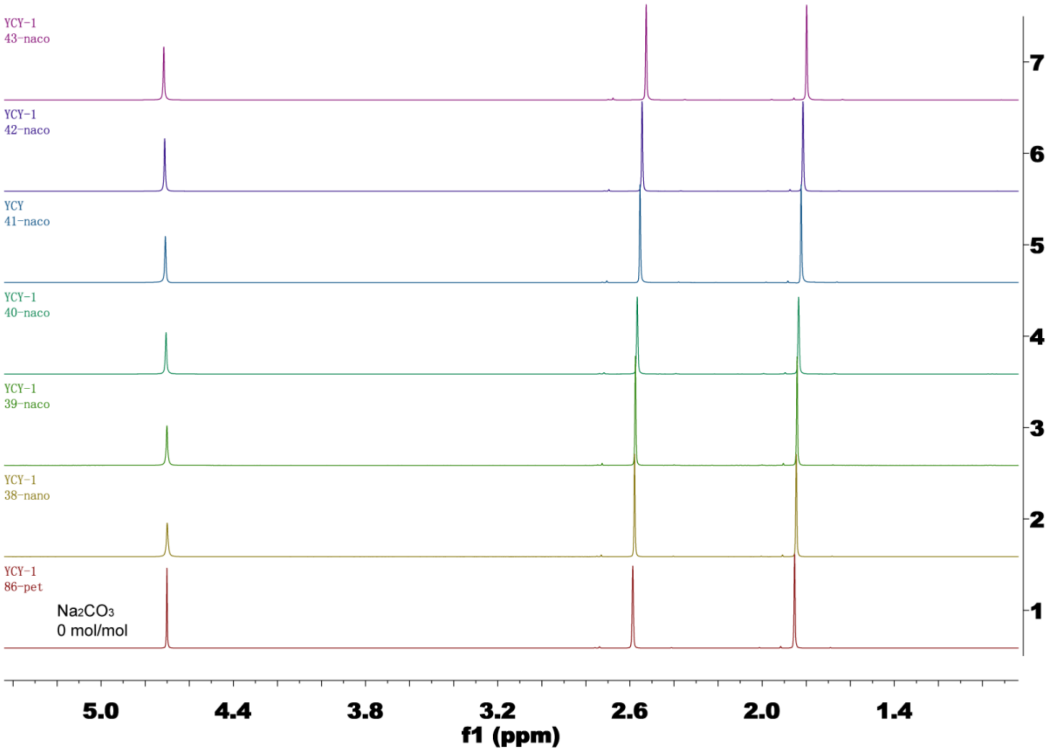

Fig. S20 Original data of Na_2CO_3 effects on NMR spectra of NMA. The concentration of NMA was constantly 0.25 M while the concentration of Na_2CO_3 in sample solutions was decreasing from upper spectra to bottom.

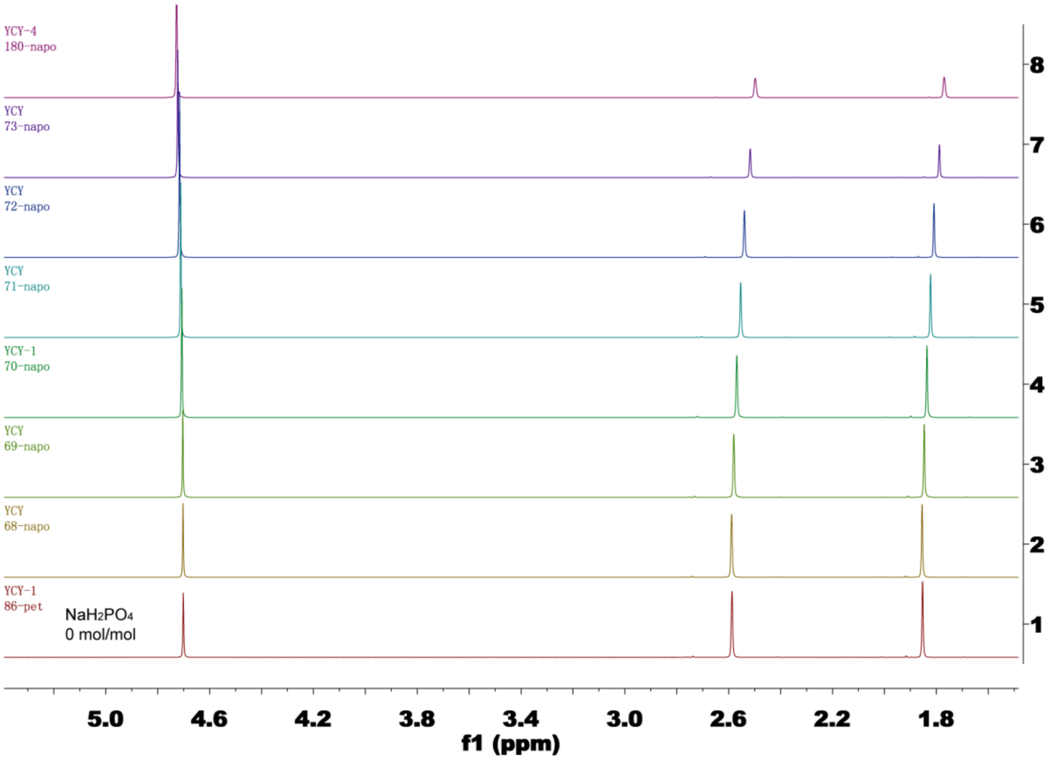

Fig. S21 Original data of NaH_2PO_4 effects on NMR spectra of NMA. The concentration of NMA was constantly 0.25 M while the concentration of NaH_2PO_4 in sample solutions was decreasing from upper spectra to bottom.

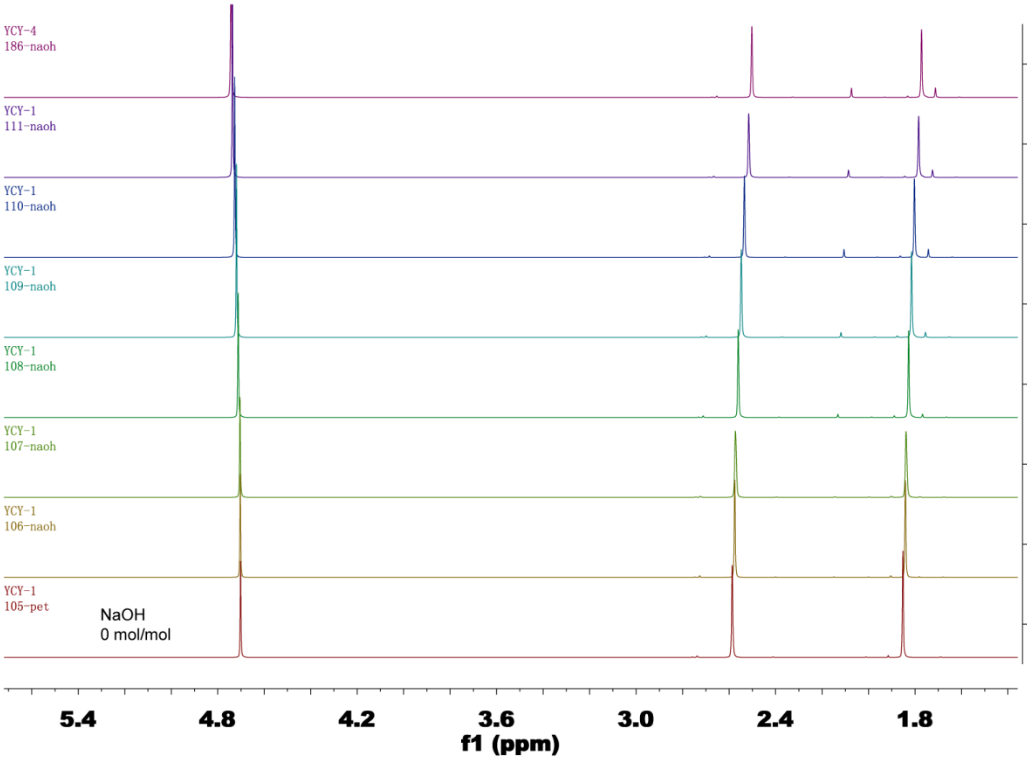

Fig. S22 Original data of NaOH effects on NMR spectra of NMA. The concentration of NMA was constantly 0.25 M while the concentration of NaOH in sample solutions was decreasing from upper spectra to bottom.

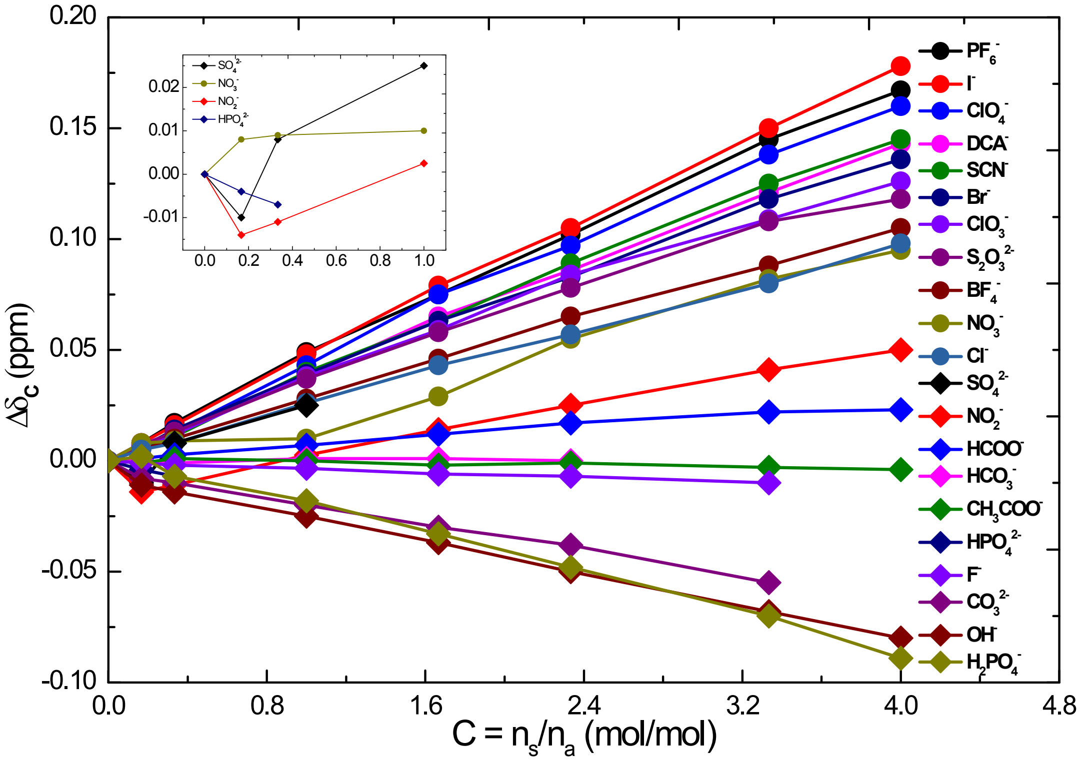

Fig. S23 Anionic effects on proton C of NMA when the cations are Na^+. A nearly linear relationship exists between the changes in the chemical shift for C proton of NMA, and concentration of anions. The inserted figure is the enlarged display of the whole figure at the concentration from o to 1.0 mol/mol.

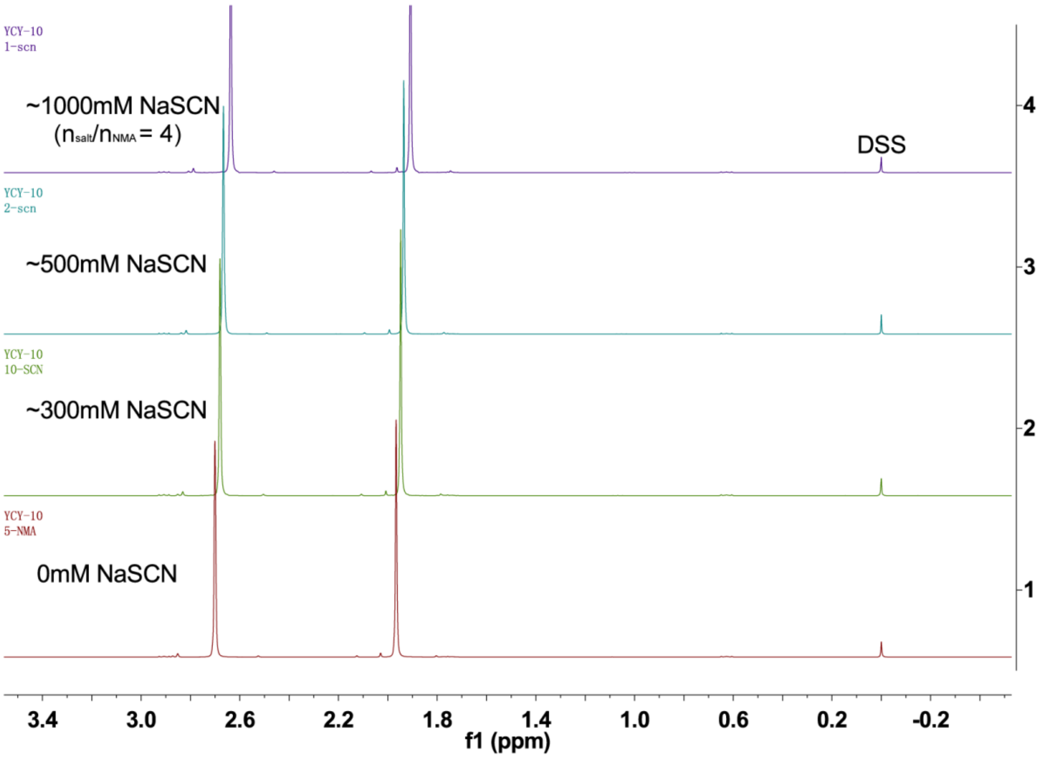

Fig. S24 Original data of NaSCN effects on NMR spectra of NMA with DSS/D_2O loaded in capillary tube as external reference. The concentration of NMA was constantly 0.25 M while the concentration of NaSCN in sample solutions was decreasing from upper spectra to bottom.

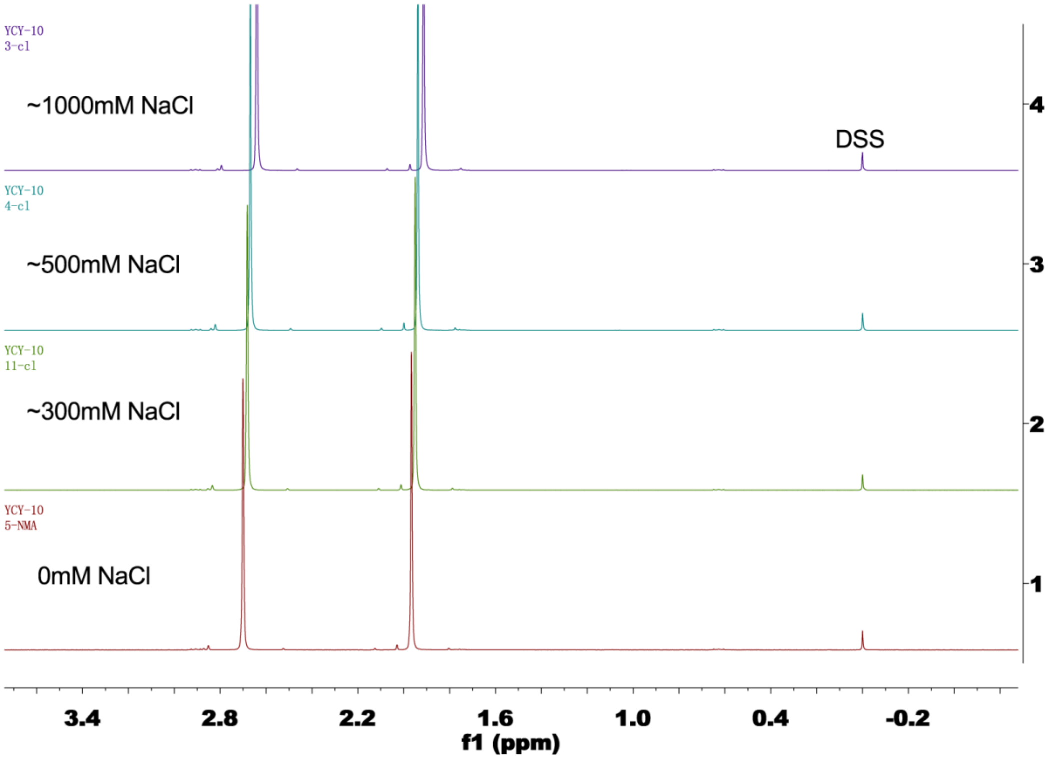

Fig. S25 Original data of NaCl effects on NMR spectra of NMA with DSS/D_2O loaded in capillary tube as external reference. The concentration of NMA was constantly 0.25 M while the concentration of NaCl in sample solutions was decreasing from upper spectra to bottom.

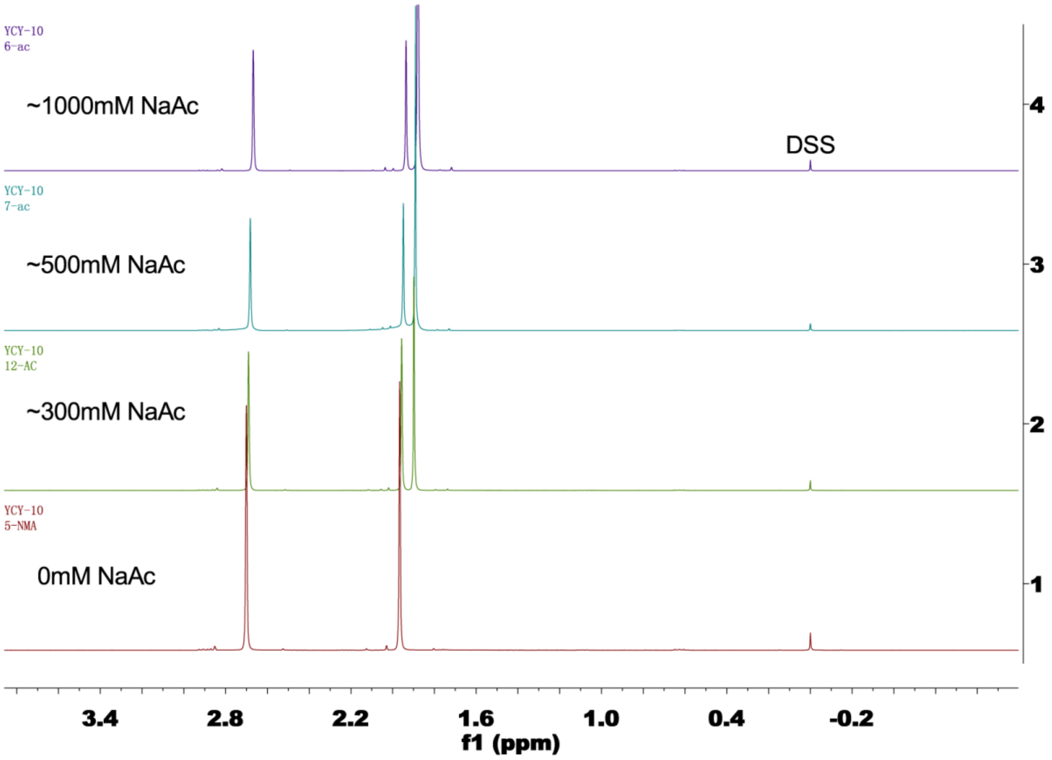

Fig. S26 Original data of $NaOOCCH_3$ effects on NMR spectra of NMA with DSS/D_2O loaded in capillary tube as external reference. The concentration of NMA was constantly 0.25 M while the concentration of $NaOOCCH_3$ in sample solutions was decreasing from upper spectra to bottom.

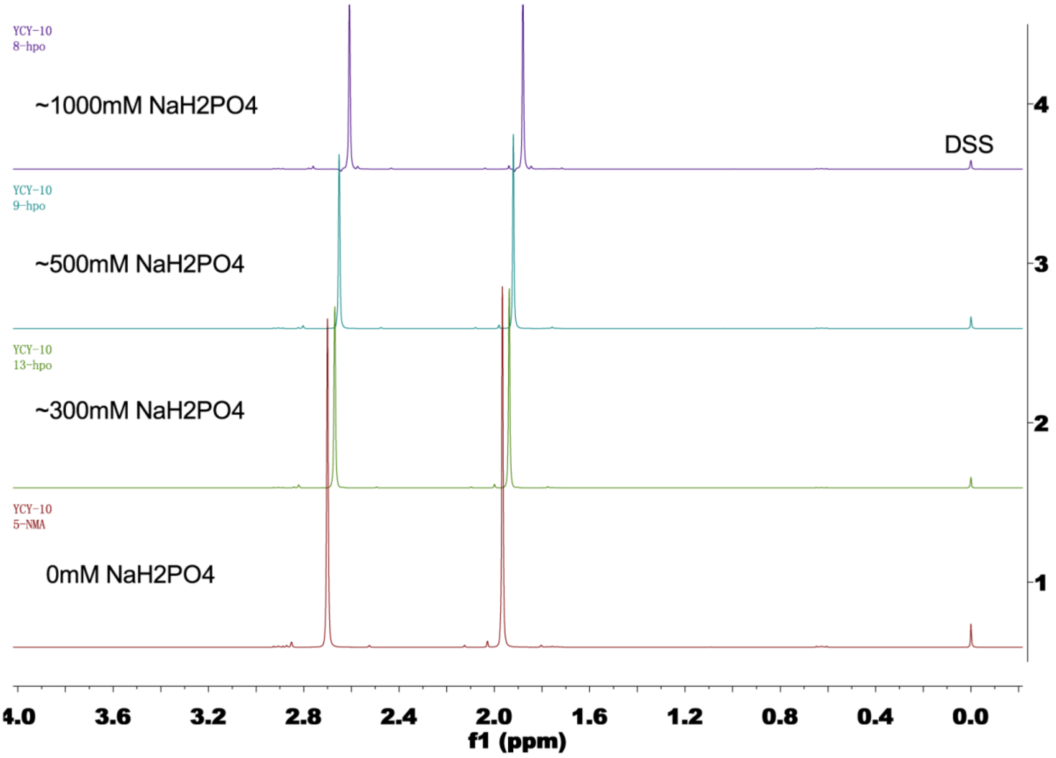

Fig. S27 Original data of NaH_2PO_4 effects on NMR spectra of NMA with DSS/D_2O loaded in capillary tube as external reference. The concentration of NMA was constantly 0.25 M while the concentration of NaH_2PO_4 in sample solutions was decreasing from upper spectra to bottom.

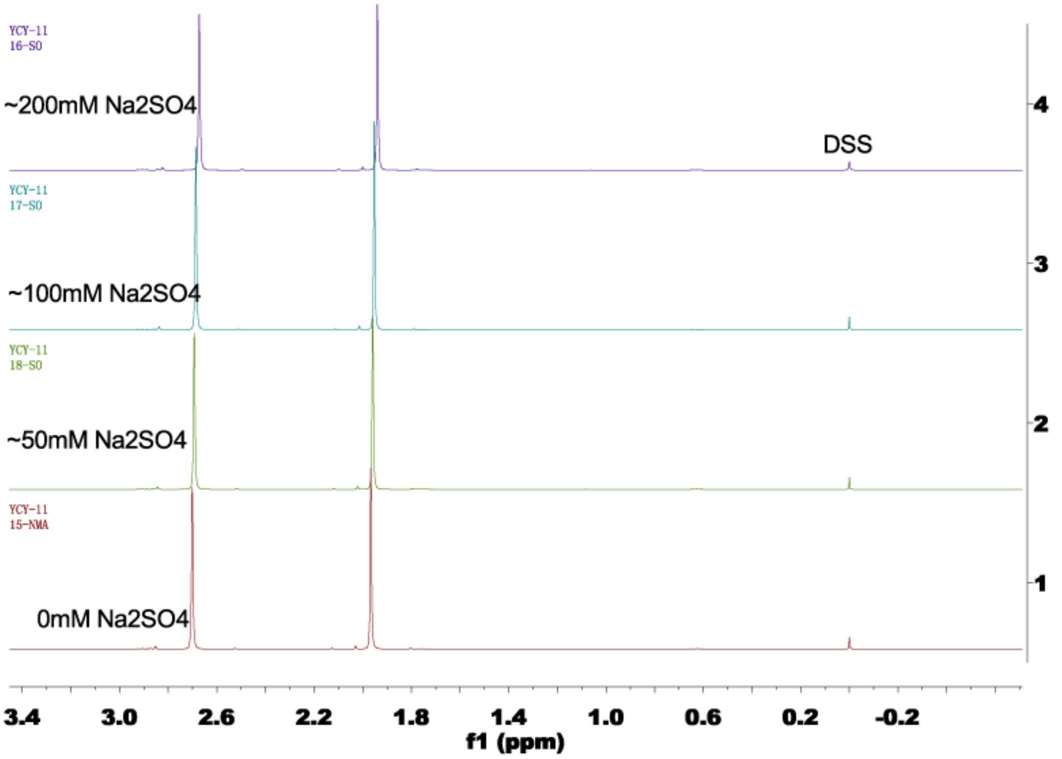

Fig. S28 Original data of Na_2SO_4 effects on NMR spectra of NMA with DSS/D_2O loaded in capillary tube as external reference. The concentration of NMA was constantly 0.25 M while the concentration of Na_2SO_4 in sample solutions was decreasing from upper spectra to bottom.

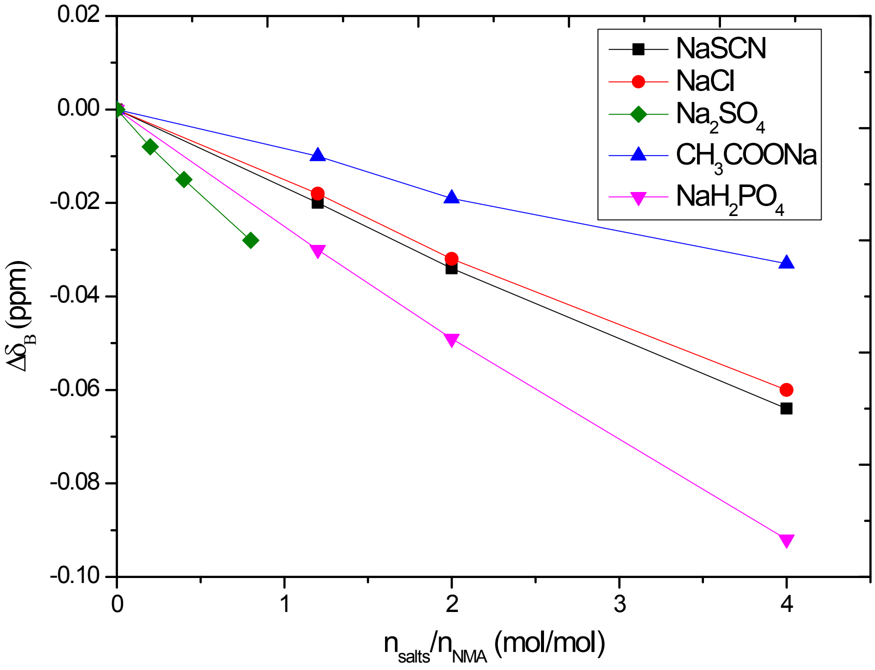

Fig. S29 Plot of concentration against changes in chemical shifts of anionic effects on NMA with DSS/D_2O loaded in capillary tube as external reference.

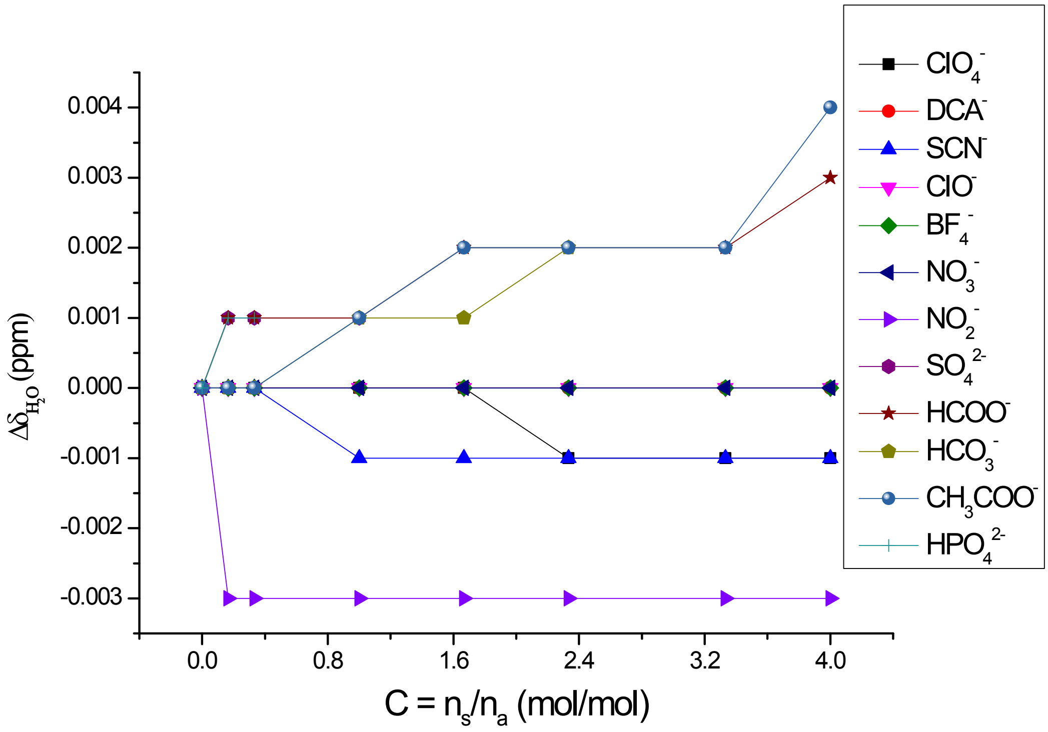

Fig. S30 Anionic effects on water residue. Changes in chemical shift for proton of water residue at different concentrations by specific anions.

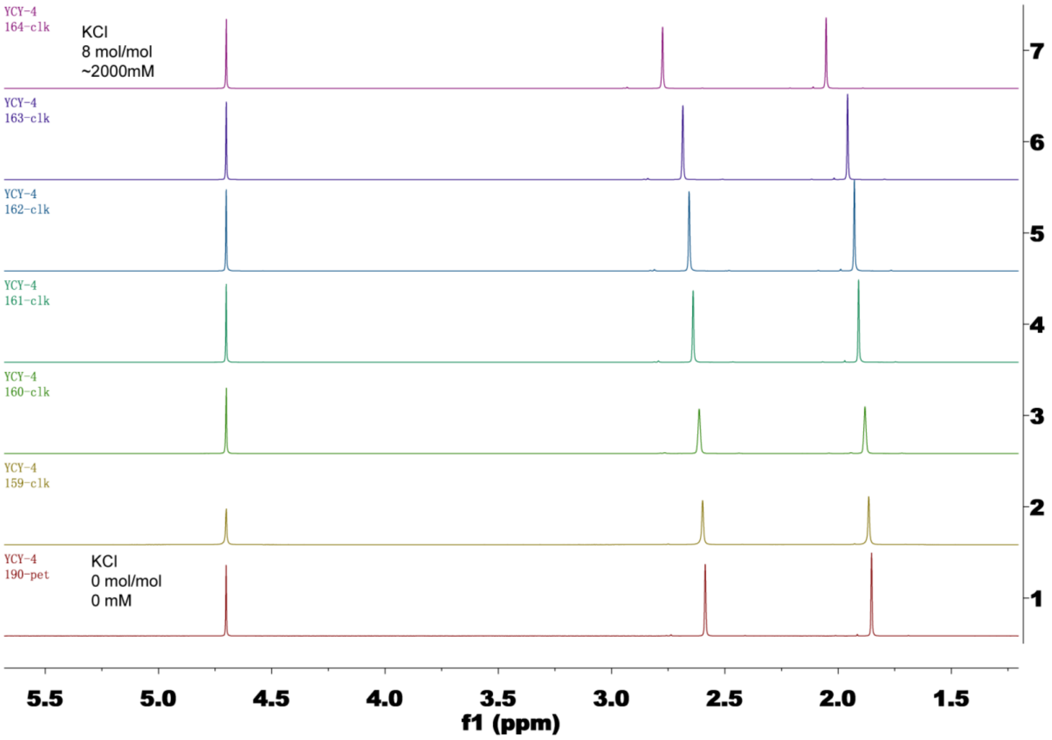

Fig. S31 Original data of KCl effects on NMR spectra of NMA. The concentration of NMA was constantly 0.25 M while the concentration of KCl in sample solutions was decreasing from upper spectra to bottom.

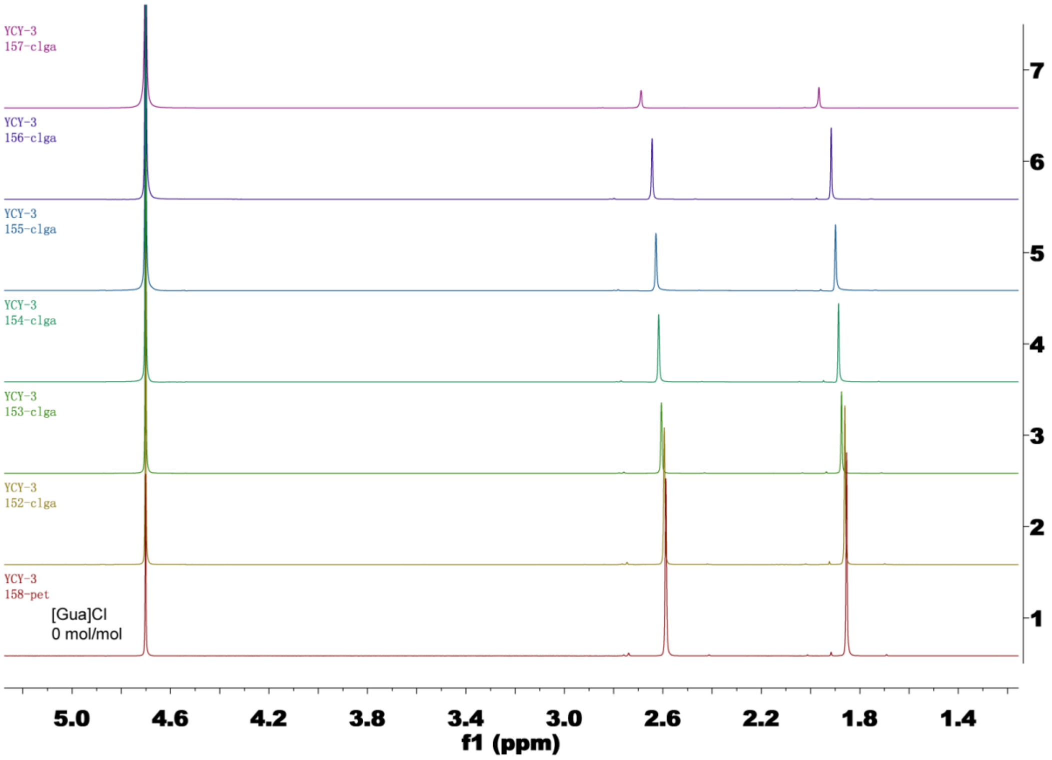

Fig. S32 Original data of Guanidine hydrochloride ([Guanidium]Cl) effects on NMR spectra of NMA. The concentration of NMA was constantly 0.25 M while the concentration of [Guanidium]Cl in sample solutions was decreasing from upper spectra to bottom.

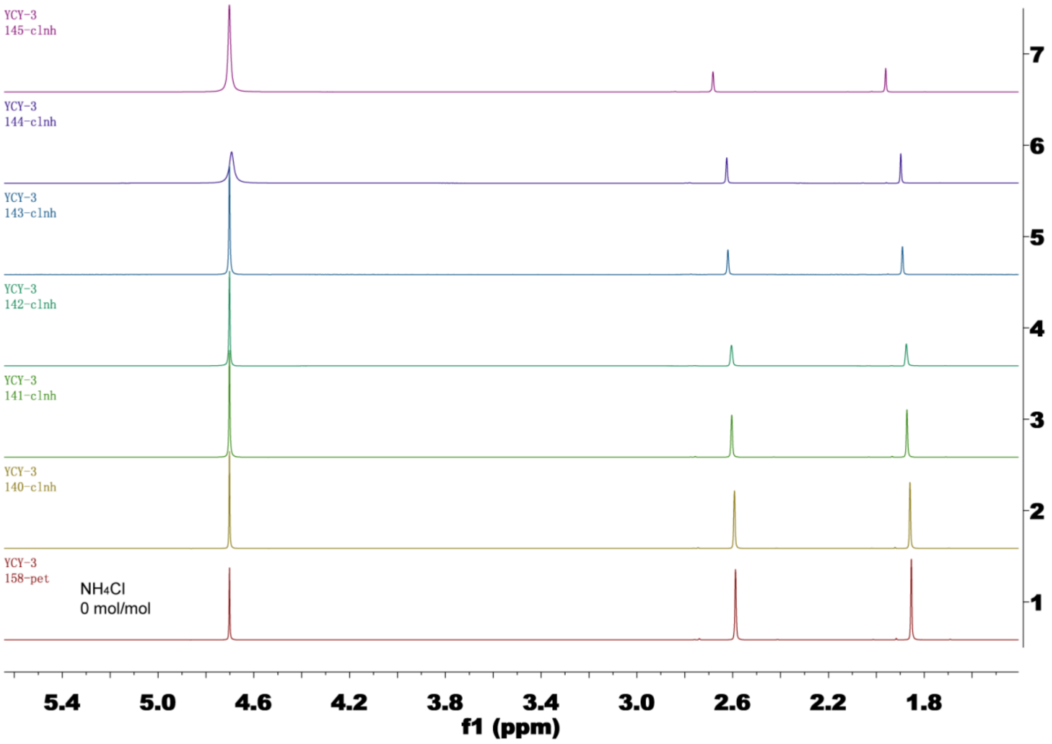

Fig. S33 Original data of NH_4Cl effects on NMR spectra of NMA. The concentration of NMA was constantly 0.25 M while the concentration of NH_4Cl in sample solutions was decreasing from upper spectra to bottom.

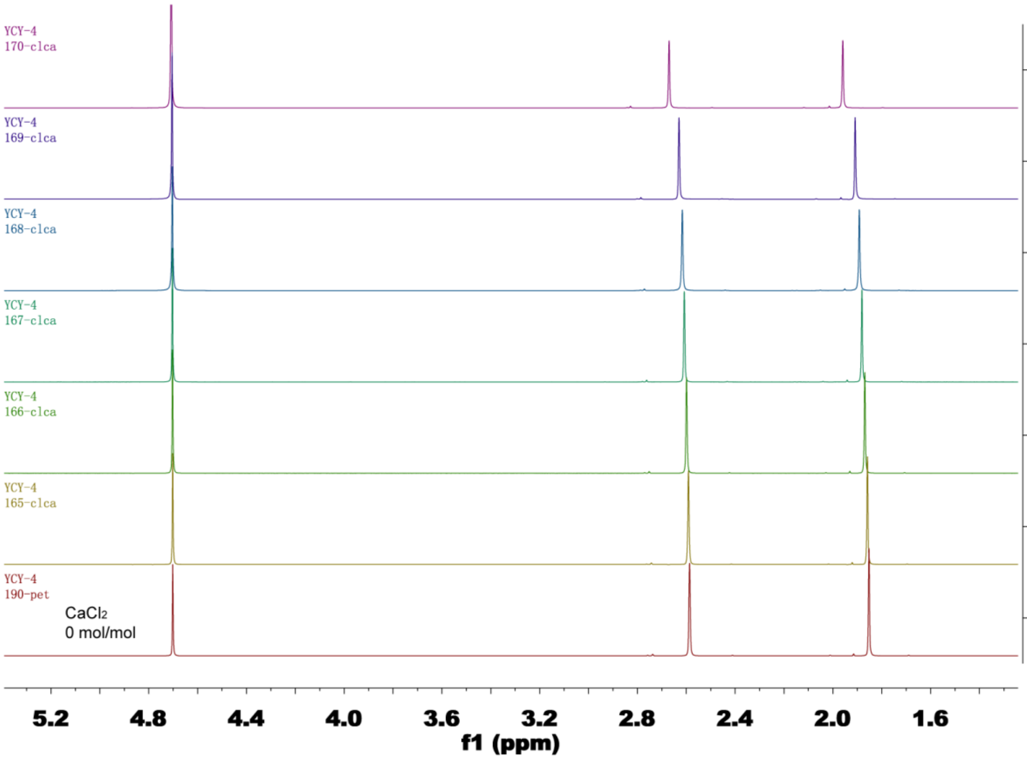

Fig. S34 Original data of $CaCl_2$ effects on NMR spectra of NMA. The concentration of NMA was constantly 0.25 M while the concentration of $CaCl_2$ in sample solutions was decreasing from upper spectra to bottom.

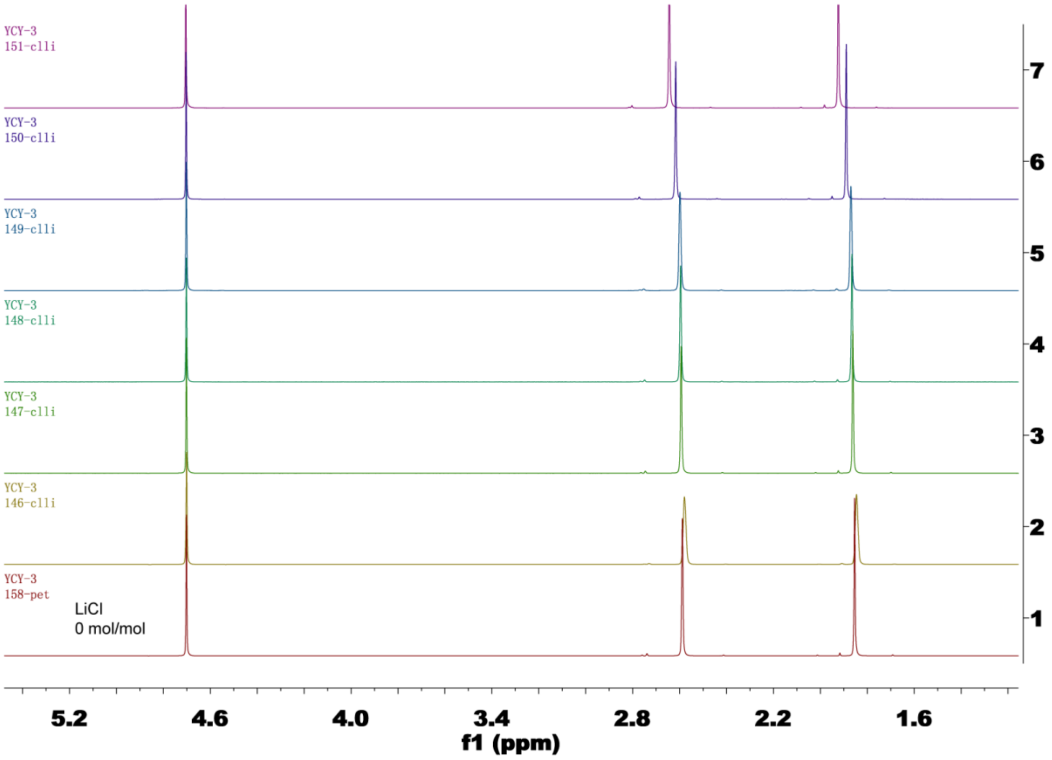

Fig. S35 Original data of LiCl effects on NMR spectra of NMA. The concentration of NMA was constantly 0.25 M while the concentration of LiCl in sample solutions was decreasing from upper spectra to bottom.

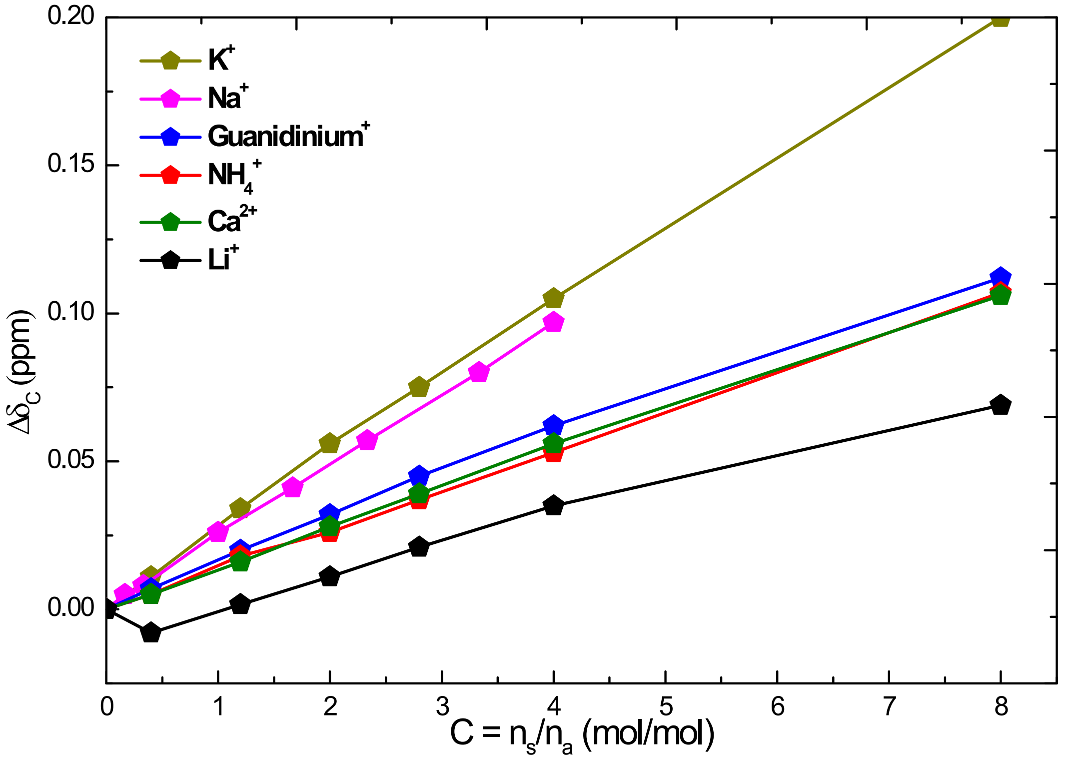

Fig. S36 Cationic effects on proton C of NMA when anions are Cl^-. A nearly linear relationship exists between the changes in the chemical shift for C proton of NMA, and concentration of cations.

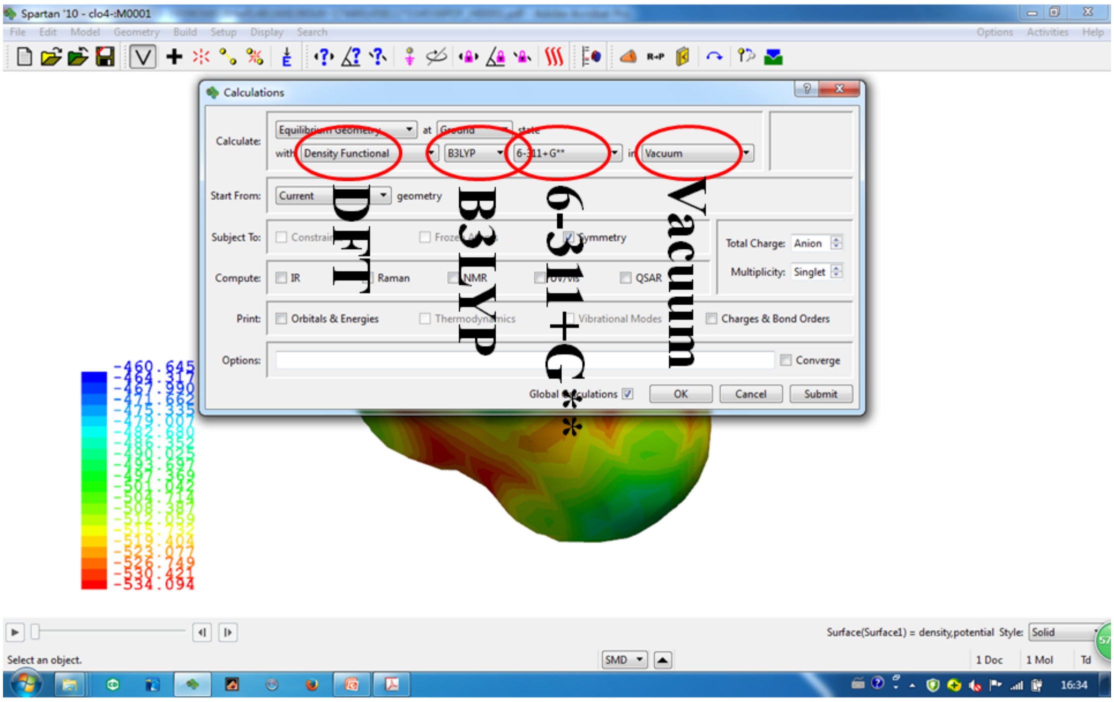

Calculate: Equilibrium Geometry at Ground state with Density Functional B3LYP 6-311+G** in Vacuum

Start From: Current geometry

Subject To: ☐ Constraints ☐ Frozen Atoms ☑ Symmetry

Compute: ☐ IR ☐ Raman ☐ NMR ☐ UV/vis ☐ QSAR

Total Charge: Anion

Multiplicity: Singlet

Print: ☐ Orbitals & Energies ☐ Thermodynamics ☐ Vibrational Modes ☐ Charges & Bond Orders

Options: ☐ Converge

Global Calculations ☑

Surface(Surface1) = density,potential Style: Solid

Select an object.

Fig. S37 Setup of calculations: calculating items at DFT/B3LYP/6-311+G** in vacuum environment with Spartan Software.

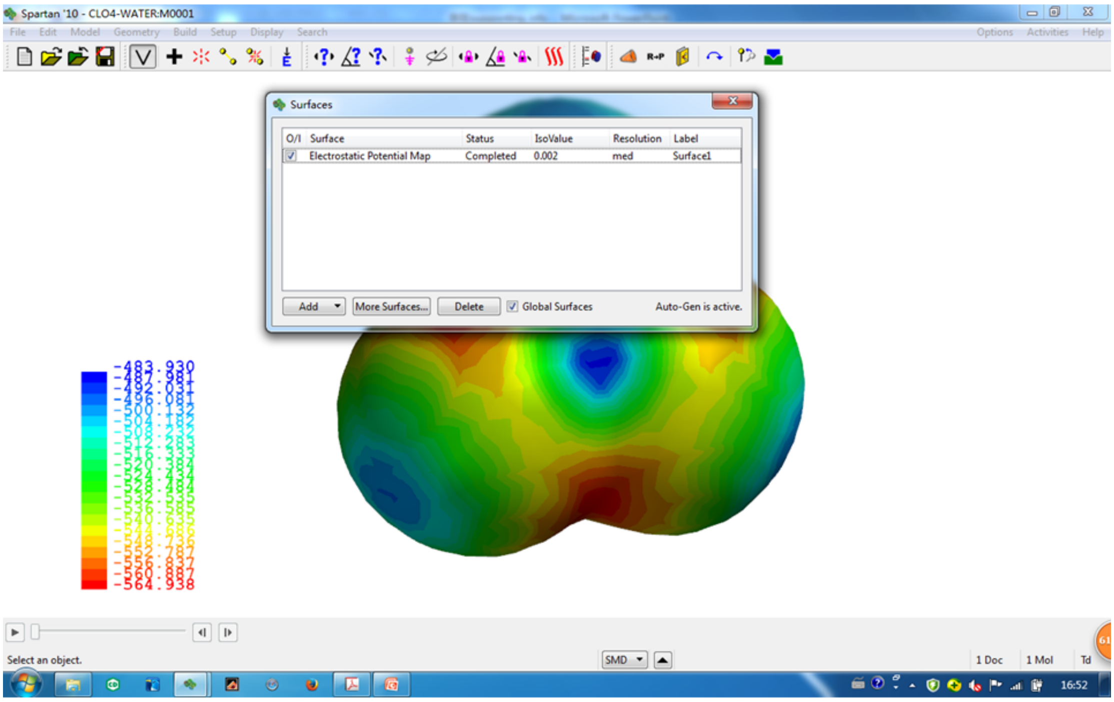

O/I	Surface	Status	IsoValue	Resolution	Label
☑	Electrostatic Potential Map	Completed	0.002	med	Surface1

☑ Global Surfaces

Auto-Gen is active.

Select an object.

Fig. S38 Displaying of electrostatic potential map.

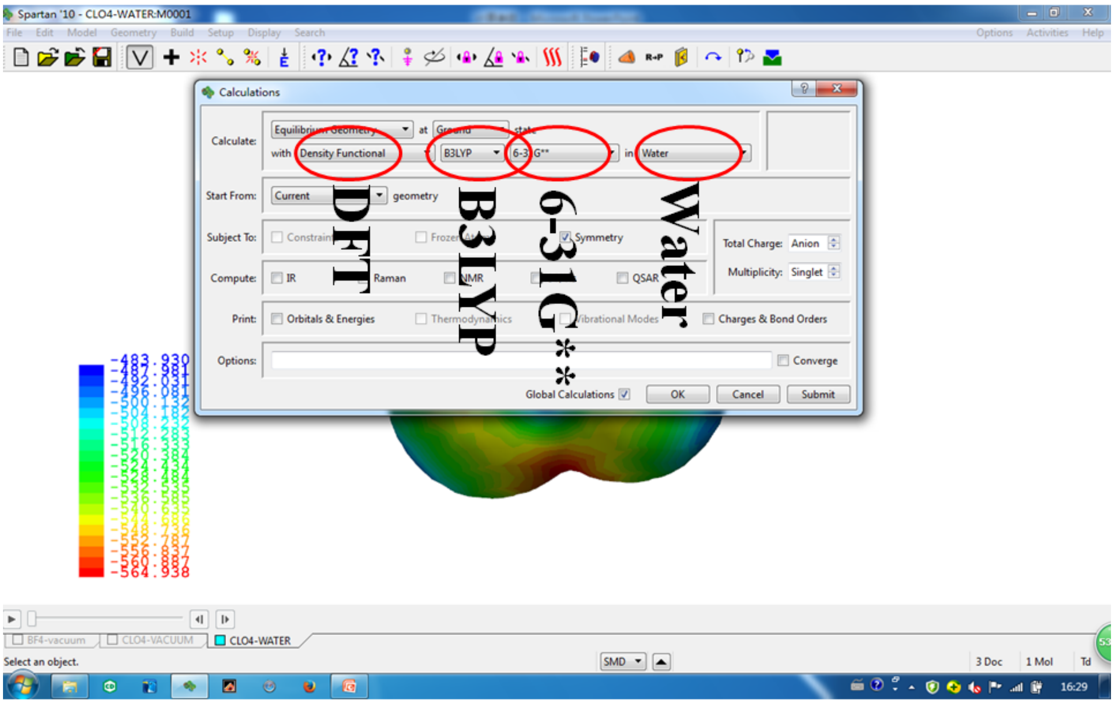

Calculate: Equilibrium Geometry at Ground state with Density Functional B3LYP 6-31G** in Water

Start From: Current geometry

Subject To: ☐ Constrain ☐ Frozen ☑ Symmetry

Total Charge: Anion

Multiplicity: Singlet

Compute: ☐ IR ☐ Raman ☐ NMR ☐ QSAR

Print: ☐ Orbitals & Energies ☐ Thermodynamics ☐ Vibrational Modes ☐ Charges & Bond Orders

Options: ☐ Converge

Global Calculations ☑ OK Cancel Submit

Fig. S39 Setup of calculations: calculating items at DFT/B3LYP/6-31G** in water environment with Spartan Software.

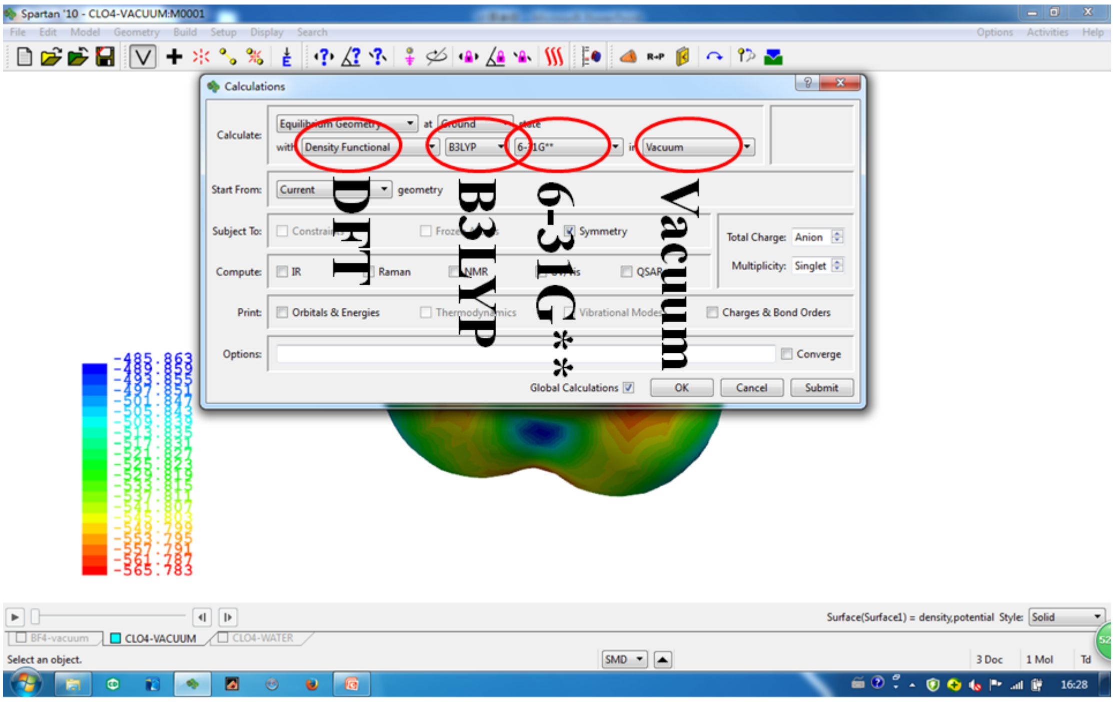

Calculations

Calculate: Equilibrium Geometry at Ground state with Density Functional B3LYP 6-31G** in Vacuum

Start From: Current geometry

Subject To: ☐ Constraints ☐ Frozen Atoms ☑ Symmetry

Total Charge: Anion

Multiplicity: Singlet

Compute: ☐ IR ☐ Raman ☐ NMR ☐ UV/vis ☐ QSAR

Print: ☐ Orbitals & Energies ☐ Thermodynamics ☐ Vibrational Modes ☐ Charges & Bond Orders

Options: ☐ Converge

Global Calculations ☑

Surface(Surface1) = density,potential Style: Solid

Select an object.

Fig. S40 Setup of calculations: calculating items at DFT/B3LYP/6-31G** in vacuum environment with Spartan Software.

Table. S1 Data of electrostatic potential surfaces in vacuum and water environments.

Entry	Item	EPS[a] (KJ/mol)		Difference (%) = $\lvert(EPS^{water} - EPS^{vacuum})/EPS^{vacuum}\rvert$	Difference (%) = $\lvert(EPS_{vac}^{6\text{-}31G^{**}} - EPS_{vac}^{6\text{-}311+G^{**}})/ EPS_{vac}^{6\text{-}311+G^{**}}\rvert$
		In vacuum	In water		
1	PF_6^-	(**-548.3**, -467.3)	(**-549.3**, -467.5)	0.2	7
2	I^-	NA[b]	NA	-	-
3	ClO_4^-	(-565.8, -485.9)	(-564.9, -483.9)	0.2	6
4	DCA^-	(-551.7, -424.5)	(-556.4, -418.1)	0.9	2
5	SCN^-	(-580.7, -448.7)	(-597.6, -432.2)	3	2
6	Br^-	(-633.4, -627.7)	(-633.4, -627.7)	0	6
7	ClO_3^-	(-640.8, -403.6)	(-655.8, -374.1)	2	6
8	$S_2O_3^{2-}$	(-1062.4, -836.8)	(-1062.5, -823.4)	0	7
9	BF_4^-	(-616.1, -534.5)	NA	-	8
10	NO_3^-	(-664.9, -500.1)	(-665.6, -502.4)	0.1	6
11	Cl^-	(-680.5, -669.8)	(-680.5, -669.8)	0	7
12	SO_4^{2-}	(-1122.8, -980.0)	(-1125.4, -983.9)	0.3	7
13	NO_2^-	(-741.4, -579.8)	(-743.3, -578.8)	0.3	10
14	$HCOO^-$	(-723.7, -446.8)	(-736.9.3, -423.4)	2	5
15	HCO_3^-	(-691.0, -260.8)	(-725.1, -202.2)	5	6
16	CH_3COO^-	(-727.2, -330.1)	(-770.7, -294.2)	6	5
17	HPO_4^{2-}	(-1135.7, -689.6)	(-1171.4, -599.9)	3	6
18	F^-	(-908.8, -877.8)	(-908.8, -877.8)	0	16
19	CO_3^{2-}	(-1278.6, -1078.8)	(-1280.9, -1079.9)	0.2	10
20	H_2PO^{4-}	(-631.0, -186.5)	(-670.4, -129.5)	6	4
21	OH^-	(-865.3, -530.2)	(-874.0, -515.8)	1	9
22	K^+	(+826.5, +860.4)	NA	-	-
23	Na^+	(+1063.6, +1127.6)	NA	-	-
24	Gdm^+	(+403.0, +669.6)	(+403.1 +683.5)	0	0.5
25	NH_4^+	(+735.2, +817.8)	(+739.1, +817.6)	0.5	0.4
26	Ca^{2+}	(+1814.3, +1885.0)	NA	-	-
27	Li^+	(+1440.9, +1562.9)	NA	-	-
28	NMA	(-211.4, +209.2)	(-256.4, +255.1)	20[c]	2
29	d-NMA	(-211.4, +209.2)	(-256.8, +258.8)	20	2
30	H_2O	(-186.3, +211.2)	(-191.3, +221.7)	3	8
31	D_2O	(-186.3, +211.2)	(--191.3, +221.7)	3	8

Note: **a**. EPS stands for electrostatic potential surface, the data was recorded as "(the most positive value, the most negative value)"; **b**. NA stands for non-allowed, since some specific calculations are not possible because each basis set has its limits. For example, it's impossible for to be calculable in water environment after adding polarization function (which is represented by "+" in 6-311+G**) to water molecules because "in water environment" means the number of surrounding water molecules is infinite. And, 6-31G** is more appropriate for calculations for atom number below 30, thus it's not very reliable for iodide and bromide anion. And EPS calculations are non-allowed for metal cation and BF_4^- anion in water environment for some much more complex issues that it's impossible to clarify them in a single work. It's sadly true that there is no such a versatile basis set. However, in reality, DFT/B3LYP/6-311+G** is widely applied in calculating EPS and usually in vacuum environment. Thus, the results from DFT/B3LYP/6-311+G** are used in discussion since that the small and proportional differences between 6-311+G** and 6-31G** cause no rearrangement for anionic and cationic series, and that the tiny differences between water and vacuum environments also cause no rearrangement for anionic series; **c**. After taking hydration effects into account, the NMA molecule becomes 20% more polarized. The increment possibly results from shifts of peptide bond from type I to type II because of hydration. Nevertheless, carbonyl oxide is still more negative than oxide atoms of water so that it's still reasonable that cations such Na^+ would prefer interacting with carbonyl oxide to interacting with oxide atoms of water because larger electrostatic force. Interestingly, the proton of N-H group in NMA molecule becomes more positive than proton of water molecule in water environment whereas it is vice versa in vacuum environment. However, whether specific anion is hydrated or stays naked (in other words, goes to N-H group) largely depends on its own hydrophilcity (as a part of our goal in this study, we are trying to, to some extent, quantitatively define this abstract concept by the combination of EPS and HB terminus). Thus, under the same conditions (same NMA and same aqueous environment), there is no bias in depicting the hydrophilcity of anions by using EPS and changes in chemical shifts.

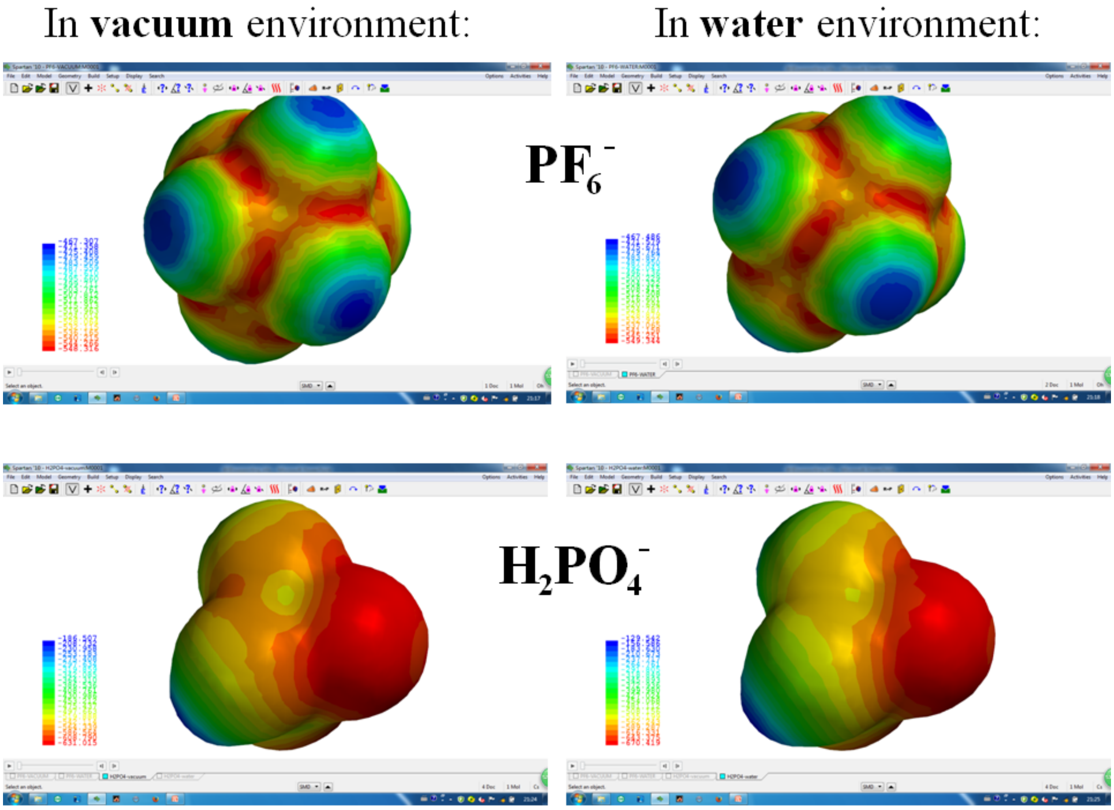

Fig. S41 Hydration effects on electrostatic potential surfaces of different anions.

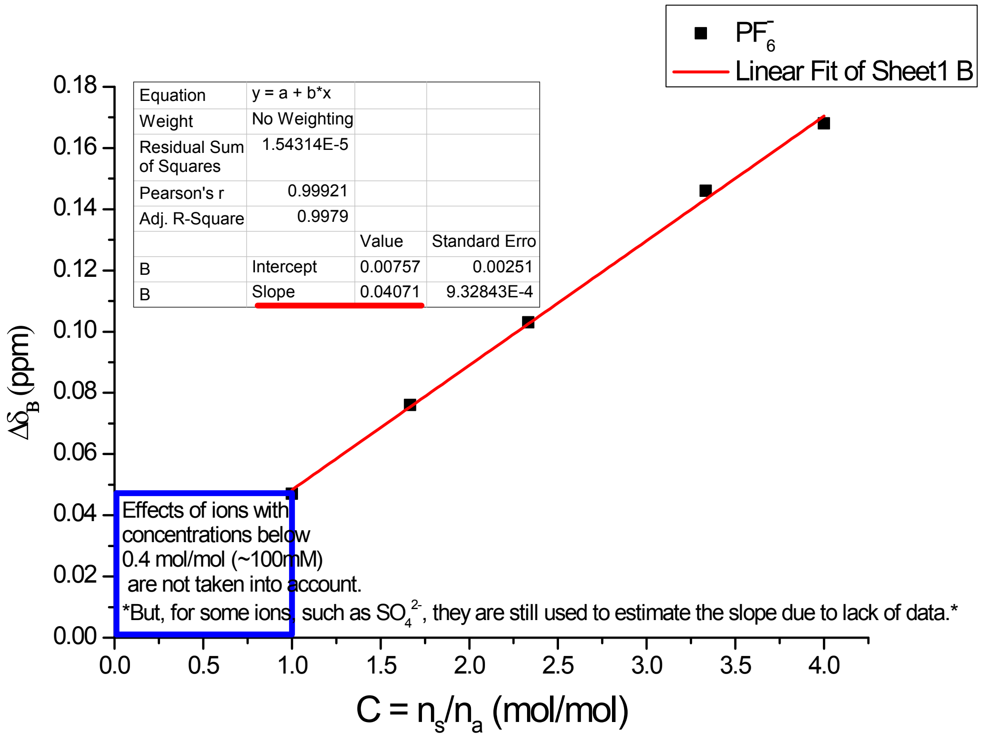

Fig. S42 An example of deriving the slope$_B$ that is the rate of changing chemical shifts under effects of ions, from Fig. 2&4.

	$\mathrm{Slope_B}$ (ppm/1)
PF6-	0.0407
I-	0.0403
ClO4-	0.0383
DCA-	0.0339
SCN-	0.0340
Br-	0.0302
ClO3-	0.0283
S2O32-	0.0253
BF4-	0.0251
NO3-	0.0288
Cl-	0.0218
SO42-	0.0270
NO2-	0.0158
HCOO-	0.0053
HCO3-	-0.0023
CH3COO-	-0.0016
HPO42-	-0.0210
F-	-0.0034
CO32-	-0.0169
H2PO4-	-0.0209
OH-	-0.0193
K+	0.0232
Na+	0.0218
Gdm+	0.0123
NH4+	0.0116
Ca2+	0.0104
Li+	0.0086

Table S2. The values of $\mathrm{slope_B}$ derived from Fig. 2&4.